

**Titre:** Mechanical Resistance of Cracked Dam Mass Concrete Repaired by  
Grouting: An Experimental Study

**Auteur:** Simon Gallagher  
Author:

**Date:** 2012

**Type:** Mémoire ou thèse / Dissertation or Thesis

**Référence:** Gallagher, S. (2012). Mechanical Resistance of Cracked Dam Mass Concrete  
Repaired by Grouting: An Experimental Study [Mémoire de maîtrise, École  
Citation: Polytechnique de Montréal]. PolyPublie. <https://publications.polymtl.ca/1013/>

 **Document en libre accès dans PolyPublie**  
Open Access document in PolyPublie

**URL de PolyPublie:** <https://publications.polymtl.ca/1013/>  
PolyPublie URL:

**Directeurs de  
recherche:** Pierre Léger  
Advisors:

**Programme:** Génie civil  
Program:

UNIVERSITÉ DE MONTRÉAL

MECHANICAL RESISTANCE OF CRACKED DAM MASS CONCRETE  
REPAIRED BY GROUTING: AN EXPERIMENTAL STUDY

SIMON GALLAGHER

DÉPARTEMENT DES GÉNIES CIVIL, GÉOLOGIQUE ET DES MINES  
ÉCOLE POLYTECHNIQUE DE MONTRÉAL

MÉMOIRE PRÉSENTÉ EN VUE DE L'OBTENTION  
DU DIPLÔME DE MAÎTRISE ÈS SCIENCES APPLIQUÉES  
(GÉNIE CIVIL)

DÉCEMBRE 2012

UNIVERSITÉ DE MONTRÉAL

ÉCOLE POLYTECHNIQUE DE MONTRÉAL

Ce mémoire intitulé:

MECHANICAL RESISTANCE OF CRACKED DAM MASS CONCRETE REPAIRED BY  
GROUTING: AN EXPERIMENTAL STUDY

présenté par: GALLAGHER Simon

en vue de l'obtention du diplôme de: Maîtrise ès sciences appliquées

a été dûment accepté par le jury d'examen constitué de :

M. CHARRON Jean-Philippe, Ph.D, président

M. LÉGER Pierre, Ph. D., membre et directeur de recherche

M. MASSICOTTE Bruno, Ph.D., membre

*This work is lovingly dedicated to*

*Syl*

## ACKNOWLEDGEMENTS

This project would not have been possible without the help and support of many people.

I would like to thank my advisor, Pierre Léger, for the long hours spent patiently discussing, reviewing and working on this project. His guidance, organization, and expertise were a continual source of motivation and helped tremendously with making this a pleasant experience.

I owe a lot of thanks to the entire team in structures laboratory. Thank you for helping me overcome all the obstacles and barriers that experimental research throws at you, without such a dedicated and willing team, none of this would have been possible.

I would like to thank to the committee members, Bruno Massicotte and Jean-Philippe Charron, for taking the time and energy to read, evaluate, and comment on this work.

Thanks are owed to National Science and Engineering Research Council of Canada (NSERC), and the Quebec Funds for Research on New Technologies (FQRNT) for financing this research work. As well, thanks are owed to Hydro-Quebec for their cooperation in providing invaluable resources and time and to Holcim for providing the injection grout.

I would also like to extend my gratitude to Marc-André Tessier whose help was invaluable.

Thank you to my friend and family who support and presence was always made available to me.

Thank you to my parents, Richard and Elizabeth, who have always encouraged me to eagerly follow my passion and who taught me what one can accomplish with hard work.

Last but not least, I would like to thank my girlfriend and best friend, Sylvana Hochet; who gave me constant and continuous help, love, and support; who put up with me and pushed me even when it was hard; and who made every moment that much more enjoyable. Thank you for being an amazing person. I love you.

## RÉSUMÉ

Pour évaluer le module de rupture et la résistance au cisaillement du béton de masse réparé par injection de coulis, six spécimens de 400 x 400 x 1250 mm en béton avec des agrégats de taille maximale de 100 mm ont été testés suivant la norme ASTM C78 et avec une configuration de chargement favorisant de grandes contraintes de cisaillement le long d'un plan de rupture vertical. L'essai de la norme ASTM C78 a été effectué sur tous les échantillons non-fissurés et sur les échantillons réparés (deux spécimens à réparation simple et deux à réparations multiples en utilisant deux coulis d'injection microfins avec un ratio eau/ciment (e/c) de 1,0 et 0,5 respectivement. L'essai de cisaillement a été effectué sur deux spécimens à réparation simple et deux spécimens à réparations multiples, injectés dans les deux cas avec les deux mélanges de coulis. Une résistance à la traction indirecte moyenne de 2,8 MPa a été obtenue pour les échantillons vierges. Cette valeur a été diminuée à 1 MPa et 0,5 MPa pour les échantillons réparés à l'aide du coulis avec rapport e/c égal à 0,5 et 1,0 respectivement, quel que soit le nombre de réparations. La résistance au cisaillement des spécimens est affectée à la fois par le rapport e/c du coulis d'injection et par de la largeur des fissures réparées.

**Mots-clés:** Béton de masse; injection de coulis; réparation de coulis; module de rupture; résistance en traction; résistance en cisaillement; barrage; béton à gros agrégats.

## ABSTRACT

To evaluate the modulus of rupture and the shear strength of mass concrete repaired by grout injection, six 400 x 400 x 1250 mm concrete specimens with a maximum aggregate size of 100 mm were tested following ASTM C78 and a loading configuration promoting large shear stresses along a vertical failure plane. ASTM C78 was done on the all virgin specimens and on repaired specimens (two repaired once and two repaired multiple times) using two different micro fine injection grout mixes with water cement ratio (w/c) of 1.0 and 0.5. The shear test was done on two single repaired and two multiple repaired specimens; with both grout mixes. Average indirect tensile strength of 2.8 MPa was obtained for virgin specimens. This value was reduced to 1 MPa and 0.5 MPa for specimens repaired using grout with a w/c ratio respectively equal to 0.5 and 1.0 regardless of the number of repairs. The shear strength of the specimens is affected by both the injection grouts w/c ratio and the repaired crack width.

**Keywords:** mass concrete; grout injection; crack repair; modulus of rupture; tensile resistance; shear resistance; dam; large aggregate concrete.

## TABLE OF CONTENTS

ACKNOWLEDGEMENTS .....	IV
RÉSUMÉ.....	V
ABSTRACT .....	VI
TABLE OF CONTENTS .....	VII
LIST OF TABLES .....	X
LIST OF FIGURES.....	XI
LIST OF ACRONYMS AND ABBREVIATIONS.....	XIII
LIST OF SYMBOLS .....	XIV
INTRODUCTION.....	1
CHAPTER 1    APPROACH TO THE PROJECT AND ORGANIZATION OF THE THESIS	3
1.1    Approach to the Project.....	3
1.2    Organisation of the Thesis.....	3
CHAPTER 2    LITERATURE REVIEW .....	5
2.1    Mass Concrete .....	5
2.1.1    Compressive Strength .....	5
2.1.2    Tensile Strength.....	7
2.1.3    Shear Strength .....	9
2.1.4    Multi-Axial Stress States.....	9
2.1.5    Modulus of Elasticity and Poisson's Ratio .....	10
2.1.6    Additional Considerations.....	10
2.2    Cracking in Concrete Dams .....	10
2.2.1    Causes.....	10
2.2.2    Types of Cracks in Dams .....	12



2.2.3	Repair Methods .....	12
2.3	Injection.....	13
2.3.1	Injection Grout Properties .....	13
2.3.2	Types of Grout .....	16
2.3.3	Additives and Admixtures.....	17
2.3.4	Injection Methods.....	18
2.3.5	Addition Considerations.....	21
2.4	Repair Case Studies.....	21
2.4.1	Isle Maligne Hydroelectric Power Complex .....	21
2.4.2	Sayano-Shushenskoe Hydrostation Dam .....	22
2.4.3	Daniel-Johnson Multiple-Arch Dam .....	23
2.5	Conclusion.....	24
CHAPTER 3 ARTICLE 1: MECHANICAL RESISTANCE OF CRACKED DAM MASS CONCRETE REPAIRED BY GROUTING: AN EXPERIMENTAL STUDY .....		26
3.1	Introduction .....	26
3.2	Research Significance .....	28
3.3	Experimental Investigation .....	28
3.3.1	Mass Concrete Mix and Related Properties .....	28
3.3.2	Grout Mixes and Related Properties .....	30
3.3.3	Beam Specimens .....	31
3.3.4	Testing Program .....	31
3.3.5	Modified Modulus of Rupture ASTM C78.....	32
3.3.6	Grouting Repair.....	33
3.3.7	Shear Test.....	34
3.4	Experimental Results and Discussion .....	35

3.4.1	Mass Concrete Mix and Related Properties .....	35
3.4.2	Grout Mixes and Related Properties .....	36
3.4.3	Modulus of Rupture .....	37
3.4.4	Shear Strength .....	39
3.5	Summary and Conclusions.....	40
3.6	Acknowledgments .....	43
3.7	References .....	44
CHAPTER 4	COMPLEMENTARY RESULTS AND GENERAL DISCUSSION.....	47
4.1	Development of Concrete Mix.....	47
4.2	Grout Rheology .....	53
4.3	Test Method Design .....	54
4.3.1	Direct Tension .....	55
4.3.2	Splitting Test .....	55
4.3.3	Modulus of Rupture .....	56
4.4	Injection Procedure .....	56
4.5	Complementary Load-Displacement Data .....	58
4.5.1	Modulus of Rupture .....	58
4.5.2	Shear Test .....	60
4.6	Prospective Future Work.....	62
4.6.1	Experimental .....	62
4.6.2	Numerical .....	63
CONCLUSIONS	.....	65
BIBLIOGRAPHY	.....	68

## LIST OF TABLES

Table 2-1: Relationship Between Compressive Strength and Tensile Strength of Concrete .....	8
Table 3-1: Mass Concrete Mixes .....	29
Table 3-2: Grout Mixes .....	30
Table 3-3: Specimens and Test Order .....	32
Table 3-4: Concrete Rheology .....	35
Table 3-5: Concrete Properties.....	36
Table 3-6: Grout Properties and Rheology .....	36
Table 3-7: Modulus of Rupture Test Results .....	38
Table 3-8: Shear Test Results.....	39
Table 4-1: 1967-68 BDJ Concrete Mix.....	47
Table 4-2: Mix1, 2, and 3 .....	48
Table 4-3: Sieve Analysis .....	49
Table 4-4: Small Scale Concrete Mixes .....	50
Table 4-5: Mix A.....	51
Table 4-6: Stacking Model Mixes.....	52
Table 4-7: Wet Concrete Properties .....	52
Table 4-8: Final Experimental Mix.....	53
Table 4-9: Modulus of Rupture Results .....	59

## LIST OF FIGURES

Figure 2-1: Tension Tests: (a) Direct; (b) Brazilian; (c) Modulus of Rupture; (d) Wedge Splitting .....	7
Figure 2-2: (a) Unstable Grout vs. (b) Stable Grout .....	14
Figure 2-3: Grout Intensity Number and Injection flow paths.....	20
Figure 2-4: Grouting of plunging crack: (a) BDJ dam, (b) typical concrete crack pattern, (c) reservoir level, (d) seepage Arch 5-6 .....	23
Figure 3-1: Grouting of plunging crack: (a) BDJ dam, (b) typical concrete crack pattern, (c) reservoir level, (d) seepage Arch 5-6 .....	27
Figure 3-2: Mass concrete cylindrical specimen (400mm x 800mm).....	29
Figure 3-3: Modified Modulus of Rupture – ASTM C 78.....	31
Figure 3-4: Injection and Injection Frame.....	33
Figure 3-5: Shear Test Setup: (a) Test Setup; (b) Shear Force and Bending Moment Diagram ...	34
Figure 3-6: Modulus of Rupture Failure Plane (Specimen E) .....	37
Figure 3-7: Force vs. Displacement of Virgin Specimens (A to F) .....	38
Figure 3-8: Force vs. Displacement of Repaired Specimens (A (grout w/c) and B (grout w/c)....	38
Figure 3-9: Shear Failure Plane: (a) vertical failure plane – Specimen B; (b) inclined failure plane – Specimen D .....	40
Figure 4-1: Granulometric Curve .....	49
Figure 4-2: 28 Day $f'_c$ (small scale mix).....	50
Figure 4-3: Grout-Rheological tests: (a) Bleeding, (b) Cone Marsh, (c) Thermocouple.....	53
Figure 4-4: Typical Thermocouple Results.....	54
Figure 4-5: Injection: (a) Injection Flow Path, (b) Injection Frame.....	57
Figure 4-6: Modulus of Rupture Instrumentation .....	58
Figure 4-7: Crack Opening: (a) Bottom/Top, (b) North/South .....	60

Figure 4-8: Shear Test Instrumentation.....	60
Figure 4-9: Load vs. Deformation: (a) Crack Opening B, (b) Center Deflection B, (c) Overhang B, (d) Crack Opening D, (e) Center Deflection D, (f) Overhang D.....	61
Figure 4-10: Potential Future Shear Test with Normal Force.....	62
Figure 4-11: Potential Future Bi and Tri Axial Test.....	63

## **LIST OF ACRONYMS AND ABBREVIATIONS**

### **Acronyms**

ACI	American Concrete Institute
ASTM	American Standard Test Method
GIN	Grout Intensity Number
ICOLD	International Committee on Large Dams
RTCG	Real Time Control Grouting
UDEC	Universal Distinct Element Code

### **Abbreviations**

BDJ	Daniel-Johnson Dam
LP	Linear Potentiometer
LVDT	Linear Variable Displacement Transducer
W/C	Water/Cement

## LIST OF SYMBOLS

$A$	Shear Area
$c$	Conversion Constant OR Cohesion
$f_c$	Compressive Stress
$f_r$	Third Point Bending Tensile Test Tension Stress (Modulus of Rupture)
$f_{sp}$	Splitting Tensile Test Tension Stress (Brazilian)
$f_t$	Direct Tensile Test Tension Stress
$N$	Normal Force
$\mu$	Coefficient of Friction
$\tau$	Shear Stress
$\phi$	Angle of Friction

## INTRODUCTION

Hydroelectric concrete dams are large complicated mass concrete structures that are prone to cracking. It is essential that the proper upkeep be done so that these structures are kept and maintained in safe working order. To this end, the cracks that are formed in dams must be repaired. Many different types of repair techniques exist; however, injection grouting is the most common form of dam crack repair. The study of grout injection has mainly focused on, to date, the injection grout used in repairs: rheology, cured properties such as compressive and tensile strengths, and on the distribution and penetrability of the grout during an injection. Although injection grouting has been taking place for many years, there is still little research on the mechanical tensile and shear strengths of repaired sections of mass concrete.

### Research Problem

To date, the best way to ascertain the quality of a grout injection repair in a dam is by taking a core of the repaired concrete. In the case of dam mass concrete, this may prove problematic. The first problem is that it is not always possible or convenient to obtain a core of the repaired section of dam. Additionally, given the size of the aggregates used, it would not be possible to take a core which is large enough in diameter to determine the actual strength of the repaired section (ASTM, 2002c).

This problem exists with all repaired mass concrete structures. For the purpose of this research, it was decided to focus the study on a successful repair of a crack network of a single arch of a multiple arch dam.

The Daniel-Johnson Dam (BDJ) located in the Manicouagan River in Quebec, Canada, is the largest multiple arch dam in the world. The 214 m tall dam consists of 13 cylindrical arches being supported by 14 buttresses, with a crest length of 1300m (Tahmazian, Yeh, & Paul, 1989).

Shortly after construction, many different types of cracks developed in the dam. The Dam underwent many grout repair campaigns to minimize seepage and to remove uplift pressure. Of particular interest is the repair of the plunging cracks in the arch 5-6 of the dam. The repairs undertaken proved successful in stopping virtually all the seepage in the arch. The problem is that, although the cracks are repaired, to date there is no information on tensile and shear strength that these repairs provide. Because of this lack of information, the numerical models developed to



predict the structural stability for different reservoir elevation (including Flood) assume that the grouted cracked zone provides no tensile or shear strength. This leads to a potential loss in maximum volume reservoir capacity (Saleh et al., 2003).

### **Goal and Objectives**

The main goal of this experimental research is to determine the mechanical resistance of a section of mass concrete that has been repaired by grout injection. A focus was put on trying to replicate the repairs seen in the 5-6 arch of BDJ.

To this end, the following objectives were established:

- Develop a mass concrete mix that is representative of the BDJ concrete (maximum aggregate size of 150 mm & compressive resistance of 33MPa) (Bulota, Im, & Larivière, 1991);
- Develop an experimental setup capable of determining the tensile stress of mass concrete and grouted mass concrete specimens (400 x 400 x 1200 mm);
- Develop an experimental setup capable of determining the shear resistance of grouted mass concrete specimens (400 x 400 x 1200 mm);
- Develop an experimental setup capable of injecting repair grout to the failure plane and maintaining the grout under a constant pressure until it has cured;
- Quantify the tensile resistance of an un-cracked specimen, a specimen repaired with stable grout ( $w/c = 0.5$ ), and a specimen repaired with unstable grout ( $w/c = 1.0$ );
- Quantify the shear resistance of a specimen repaired with stable grout ( $w/c = 0.5$ ) and unstable grout (1.0);
- Quantify the effects of multiple repairs on tensile resistance and shear resistance;
- Use the results obtained to make recommendations on the residual resistance of repaired concrete in both tension and shear.

The following chapter will describe the general approach taken for this experimental research and will define the organisation of the thesis

## **CHAPTER 1      APPROACH TO THE PROJECT AND ORGANIZATION OF THE THESIS**

The previous chapter identified the research problem and the objectives. The approach taken in the project to meet these objectives is described in this chapter.

### **1.1 Approach to the Project**

Initially, the first step is data acquisition. To this end, a liaison with Hydro-Quebec was needed. The communications that took place served to gather information on the history of the Daniel-Johnson dam, the cracks that occurred, and the repair methods that have been used. Detailed injection plans and injections reports were acquired. Moreover, ideas on the relevant information needed and on research plans were exchanged. The communications with Hydro-Quebec were a constant throughout the course of the project.

An extensive literature review was done to determine what has been done on this front so far. The literature review covered, mass concrete, causes for cracking in dams (thermal stress, chemical attacks, hydrostatic overload), the types of cracks seen, and repair methods used. It then examines grout properties (both liquid and cured) such as viscosity and compressive strength. The previous research on grout injection in general and specifically on mass concrete dams was reviewed and discussed. Lastly, three case studies of grout injections for dam repairs were overviewed.

To complete the objectives, the first step was to determine a facility capable and willing to produce our mass concrete mix. In tandem with the development of the mix, the testing methods to obtain the tensile and shear strengths were developed and a testing protocol was established. Once completed, the specimens were tested and the data obtained was analysed.

The results and main conclusions can be found in Chapter 3 a technical paper that was written and submitted to American Concrete Institute Structural Journal in November 2012.

### **1.2 Organisation of the Thesis**

This thesis starts with an introduction, which briefly describes the subject and highlights the issues that need further attention. Chapter 1 is a transitory summary of the approach taken for the project as well as the organisation of the memoire. Chapter 2 presents an extensive literature

review. Chapter 3 is the paper entitled “Mechanical Resistance of Cracked Dam Mass Concrete Repaired by Grouting: an Experimental Study” which was submitted to ACI. Chapter 4 is comprised of complimentary data not found in the article as well as some general discussion. A conclusion on the project follows can be found after Chapter 4.

## **CHAPTER 2      LITERATURE REVIEW**

The objective of this research project is to evaluate the effectiveness of grout injection repairs to cracks in unreinforced concrete dams. More specifically, it is to evaluate the tensile strength and shear strength of a repair done with microfine cement grout with water to cement (w/c) ratio of 0.5 and 1.0. Determining the effects of multiple repairs was also a consideration. To be able to properly draw any conclusions from any experimental study it was important to first understand the elements discussed in the literature review. The first element discussed is mass concrete, what it is, its different properties, and how those properties are tested. The mechanics of dam cracking and dam crack repair are then addressed. Injection repairs, and the injection materials are then examined in detail. Finally three case studies dams repaired by grout injection are reviewed: Isle Maligne gravity dam (43 m), Sayano-Shushenskoe dam (242 m), and Daniel-Johnson multiple-arch Dam (215 m).

### **2.1 Mass Concrete**

Mass concrete is considered to be concrete that is cast in place in such large volumes that special precautions need to be taken to control excessive temperatures and the effect that these temperatures will have on the final cured concrete. Generally mass concrete has larger than average aggregate sizes including crushed rock. The maximum aggregates usually vary between 80 mm and 150 mm although it is possible to use smaller or larger maximum aggregate sizes. Moderate-heat or low-heat cement, with additives and admixtures to control temperature are typically used for dam construction (ACI-Committee-207, 1970).

The compressive strength of dam mass concrete can range from 20 MPa to 40 MPa after 90 days. The modulus of elasticity of concrete dams at 90 days is typically found to be between 30 and 45 GPa. Poisson's ratio for mass concrete normally varies between 0.15 and 0.25 (ACI-Committee-207, 1970).

#### **2.1.1 Compressive Strength**

The compressive strength of dam concrete is its most important property, since in dam design a great effort is put into minimizing tension and promoting stress through compression. Typically,

rapid high compressive resistance, except in certain cases, is not required for dams (ICOLD-Committee-on-Concrete-Dams, 2008).

The main element that controls tensile resistance in mass concrete is the porosity of the cement paste, which depends on the water/cement (w/c) ratio. The weakest link in concrete, and the initial cracking point, is at the interface between the aggregate and the cement matrix and the porosity at this point is what affects the strength. Because porosity is not easily measured, the w/c ratio is normally used. Lowering the w/c ratio in mass concrete will typically improve the properties of the concrete that are important for dam construction such as strength and impermeability (ICOLD-Committee-on-Concrete-Dams, 2008).

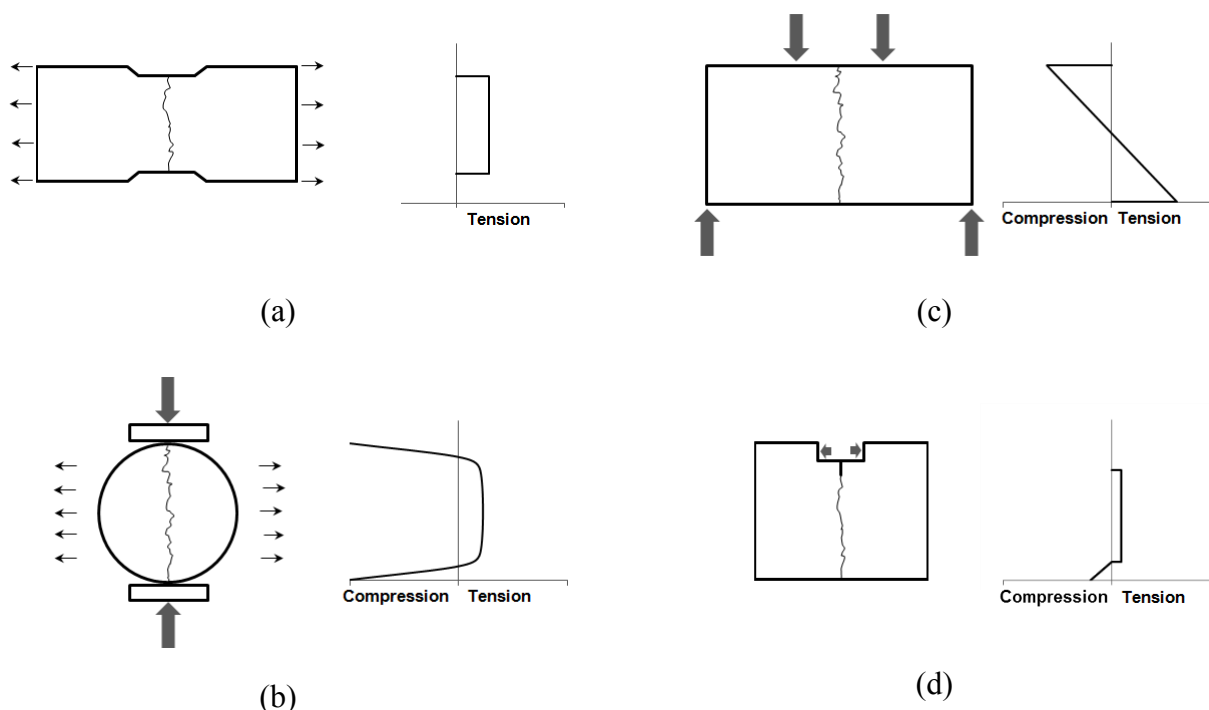
The type of aggregate, its strength, and the maximum aggregate size also play an important role in the strength of mass concrete. Typically, the strength of mass concrete is increased with increasing aggregate size. This trend can be reversed if large quantities of cement are used in the concrete mix. Additionally, as mentioned by Nallathambi, Karihaloo, and Heaton (1985), the critical energy release rate is also increased by increasing maximum aggregate size. As the aggregate strength is increased, the concrete mix using that aggregate will also show increased strength. The type of aggregate used can have varying effects on the strength of the concrete. The amount of water absorption of different rocks will have an effect on the w/c ratio used in a mix. For proper workability, certain sands also require a larger w/c ratio, which in turn has a negative effect on strength. Additionally, the cohesion between the cement matrix and different aggregates plays a role on concrete strength. This could be affected by the presence of dust on the aggregates. Lastly, the roughness of the aggregates will have an effect on the interlock found between the aggregates, which will also affect the concrete strength (ACI-Committee-207, 1970; ICOLD-Committee-on-Concrete-Dams, 2008).

The different admixtures and additives used in the concrete mix will also affect the compressive strength of the concrete mix.

It was found by Khaloo, Shooreh, and Askari (2009) that when testing mass concrete specimens, the 7 day tests are unreliable. It was also noted that the maximum aggregate size does not have a size effect factor on the test results if sufficiently large test specimens are chosen. Larger test specimens, however, tend to have lower compressive strengths.

### 2.1.2 Tensile Strength

The tensile strength of concrete dams is an important factor in determining dam safety. According to Raphael (1984), the tensile resistance of concrete is a constant property; however, the resistance measured varies depending on the method used to quantify it. The three most commonly used tests to determine tensile strength are as follows: direct tensile test,  $f_t$ ; splitting tensile test (Brazilian),  $f_{sp}$ ; and third point bending test (modulus of rupture),  $f_r$ . Much work has been done to determine the relationship between these different tensile strengths and the compressive strength of concrete. These relationships can be found in Table 2-1. The stress states caused in the specimens during the different tests can be seen in Figure 2-1 (ICOLD-Committee-on-Concrete-Dams, 2008).



Not to scale

Figure 2-1: Tension Tests: (a) Direct; (b) Brazilian; (c) Modulus of Rupture; (d) Wedge Splitting

The direct tensile test method is the least accurate of the 3 methods and shows the widest variation, as seen in the work done by Nianxiang and Wenyan (1989). This is because a small eccentricity in the application of the tensile force can dramatically affect the stresses in the specimen. Additionally, surface drying decreases the observed tensile strength dramatically for this test (Raphael, 1984).

The splitting tensile test provides the tensile strength value that is the most accurate and representative of the actual tensile strength according to Raphael (1984). For this test the effects of surface drying are negligible because, as can be seen from Figure 2-1, there are large compressive forces at the surface of the specimen, where surface drying is important, and the tension plane is located within the specimen (Raphael, 1984).

The third point loading test tends to give results that are closest to the results found in numerical modeling, which are inclined to overestimate stresses. This is due to the fact that this test model assumes, until rupture, a constant modulus of elasticity for the complete stress-strain curve. This method has less variability in results than the other two methods and the results from this test are easily reproducible (Raphael, 1984).

A fourth recently developed test method, the wedge splitting test, is advantageous because it allows for the strain softening portion of the stress-strain curve to be obtained and thus allows the fracture energy to be calculated (ICOLD-Committee-on-Concrete-Dams, 2008; Nordtest, 2005).

Table 2-1: Relationship Between Compressive Strength and Tensile Strength of Concrete

No.	Strength test	Specimens	Heilmann (1969) 'c' in: $f_t = c \cdot f_c^{2/3}$ [kg/cm <sup>2</sup> ]			Other relations (all in kg/cm <sup>2</sup> )	
			min.	avg.	max.	Source	Formula
$f_r$	Flexural: Center-point load	Prisms H: 10 cm L: various	0.86	1.07	1.28	ICOLD (2008)	$f_r = (2.5 \text{ to } 3.0) \cdot A f_c$
		As above	0.76	0.98	1.2	ICOLD (2008)	$f_r = 2.0 \cdot A f_c$
$f_r$	Flexural: Third-point load	10 x 10 x 40 cm				Khan et al. (1996)	$f_r = 0.86 \cdot f_c^{2/3}$
		cyl: 15 x 53 cm				Raphael (1984)	$f_r = 0.95 \cdot f_c^{2/3}$
$f_{sp}$	Splitting (Brazilian)	cyl: 15 x 30 cm	0.48	0.50	0.70		
$f_t$	Pure tension	cyl: 15 x 30 cm				Raphael (1984)	$f_t = 0.70 \cdot f_c^{2/3}$
		cyl: 15 x 25 cm 5 x 20 x 20 cm 9 x 15 x 60 cm	0.36	0.52	0.68	Kupfer and Gerstle (1973)	$f_t = 0.64 \cdot f_c^{2/3}$

Note: 10kg/cm<sup>2</sup> = 1 MPa; If  $f_c$  is input in MPa, multiple  $f_t$  by 0.464 for approximate value in MPa.

Adapted from ICOLD-Committee-on-Concrete-Dams (2008)

### 2.1.3 Shear Strength

The shear strength for mass concrete can be represented by the following formula:

$$\tau = c \cdot A + \mu \cdot N$$

Where:

$\tau$  = Shear Strength

$c$  = Cohesion

$A$  = Shear Area

$\mu$  = Coefficient of Friction [ $\tan(\phi)$ ].  $\phi$  = Friction Angle]

$N$  = Normal Force

The first part of the equation represents the bond between the different elements on the shear plane. It is a material property that is affected by the component of the concrete mix. The second part of the equation is simply the resistance due to friction. It is dependent on the normal force applied to the shear plane and the rugosity of the shear plane. With larger aggregates, there is better interlock between aggregates and a larger rugosity is observed on the shear plane leading to a higher shear resistance (ICOLD-Committee-on-Concrete-Dams, 2008).

The shear strength of concrete is most important when evaluating discontinuities in a dam, such as joints and cracks. On average, shear strength of mass concrete is found to be roughly 0.2 times its compressive strength, for concretes with maximum aggregate size of 38 mm (ICOLD-Committee-on-Concrete-Dams, 2008).

The fracture energy for shear tests was found by Bažant and Pfeiffer (1986) to be roughly 25 times larger than for tensile failures. This is thought to be due to the interlocking that takes place between aggregates during shear failures, which is more important than for tensile failures. This is a reason why maximum aggregate size and surface roughness is very important in shear strength (Chupanit & Roesler, 2008).

### 2.1.4 Multi-Axial Stress States

It was found by Wang and Song (2009) that the compression and tension resistance of mass concrete is stronger under uniaxial forces than under biaxial compression-tension or tri-axial



compression-tension-tension. They also proposed equations for the failure criterion of mass concrete under these multi-axial stress-states.

### **2.1.5 Modulus of Elasticity and Poisson's Ratio**

The modulus of elasticity and Poisson's ratio for mass concrete are again affected by the w/c ratio, aggregates, admixtures, and additives.

As with the strength of concrete, a decrease in w/c ratio will increase the modulus of elasticity and Poisson's ratio. When the strength of concrete increases, so does the modulus of elasticity; however, they are not directly proportional. Additionally, the modulus of elasticity of the aggregate used also plays an important role in the modulus of the mass concrete.

There is a wide variation found in the measured Poisson's ratio and modulus of elasticity of mass concrete. This is attributed to the fact that it is difficult to accurately measure the different displacements on a large heterogeneous mass concrete specimen (ACI-Committee-207, 1970).

### **2.1.6 Additional Considerations**

Shah and Kishen (2010) note that in concrete-concrete cold joints, the size effect rules, a set of equations developed to account the effect of size on specimen strength (a larger specimen will have a lower strength), developed by Bažant (1999) still hold. Additionally, it was found that the greater the difference between the concretes on either side of the cold joint, the weaker the cold joint becomes and the more brittle the failure of the specimen.

## **2.2 Cracking in Concrete Dams**

### **2.2.1 Causes**

The main reason of cracking in concrete dams is due to tensile stresses in unreinforced concrete that exceeds the tensile resistance of concrete. There are many causes for the stress states that lead to the deterioration and cracking of concrete. The most important in concrete dams are temperature changes and large temperature gradients, chemical reactions, hydrostatic overload, and hydrofracturing (Lapointe, 1997; Saleh et al., 2003; Veltrop, Yeh, & Paul, 1990).

### **2.2.1.1 Thermal Stresses**

Changes in temperature in any material will create a change in volume. If this material is not free to move, this volume change will create stresses. Thermal stresses in mass concrete are typically seen for two reasons: because of seasonal temperature cycles and because of heat released from cement hydration. Since the hydration of cement is necessary, it is not possible to avoid this heat; however, there are ways to mitigate it or counter-balance it. Normally the concrete mixes used for mass concrete have much less cement per unit volume than standard structural concrete, which reduces the amount of heat created. There are many additives and admixtures that can be used to delay or reduce the heat of hydration. It is also possible to use ice in place of water when mixing the concrete to decrease the differential between the ambient temperature and the final cured temperature of the concrete. Another technique commonly used is to pass cooling pipes throughout the concrete to help dissipate the heat created. Slight temperature changes can be acceptable; however, any large temperature change will create cracking in the dam. Seasonal changes in ambient temperature are not avoidable but their effects on the main mass of a concrete dam are not felt as much as on the surface. Generally, the cracking caused by seasonal temperature cycles will be on the surface of the structure and will not penetrate deeply into the dam (ACI-Committee-207, 1970; Lapointe, 1997).

### **2.2.1.2 Chemical Attacks**

The most common chemical reaction in concrete is the alkali-silica reaction, which is caused by the reactions between the hydroxyl ions in the water and the silica in the aggregate. This happens when a reactive aggregate is chosen and leads to expansion in concrete. This change in volume leads to tensile stresses that in turn might lead to cracking. Many other types of chemical deterioration can take place in a dam, but they are all caused by a change in volume and the stresses that this change causes (Lapointe, 1997).

### **2.2.1.3 Hydrofracture During Grouting**

Hydrofracture during the grouting of dams initiates when the pressures in the injection fluid cause stresses in the concrete that exceed the maximum allowable tensile stress of the dam concrete. When evaluating the stresses, it is important to consider both the pre-existing stresses in

the structure as well as the stresses caused by the injection (Saleh et al., 2003; Wong & Farmer, 1973).

#### **2.2.1.4 Hydrostatic Overload**

Hydrostatic overload can be caused by poor designs such as disjointedness in geometry, the structure not acting monolithically or as was intended, or due to flooding. Since every dam is unique, having different soil conditions, topographic setting, climatic conditions, and available construction materials, it is very difficult to identify all the potential problems that may arise. That is why it is often very difficult to identify the cause or causes of cracks in dams (Veltrop et al., 1990).

### **2.2.2 Types of Cracks in Dams**

There are many different types of cracks in dams. They can be horizontal or vertical, thin or thick, have a large or small area, or be any combination of the aforementioned qualities. It is often necessary to do an in-depth investigation to determine the nature of a crack. There are many methods used to characterize and map a crack. Cameras can be lowered down boreholes to visually inspect the crack or ultrasound can be used to ascertain the extent of the cracks. Cores taken from the concrete can be tested for mechanical strength and used in chemical and petrographic tests to evaluate the quality of the concrete (Jansen, 1988; Lapointe, 1997). New methods such as the use of Rayleigh waves to characterize cracks and evaluate repairs, as proposed by Aggelis, Shiotani, and Polyzos (2009) and the method of using air-coupled sensors to evaluate crack depth, as proposed by Kee and Zhu (2010) are constantly being developed and put into practice.

### **2.2.3 Repair Methods**

Cracks in dams can cause many problems including hindering the structural integrity of the structure, problems with leakage, aesthetic concerns, and durability issues. There exists many ways of repairing cracks. Depending on the nature of the crack and the reason for the repair, the most efficient repair method is chosen. Some of the methods are stitching, drypacking, post-tensioning, and grout injection. Stitching consist in connecting both sides of the crack with „U“ shaped steel pieces. This repair method can only be used if the crack mouth is accessible. It does

not close cracks; it only provides tensile resistance to the crack area. This repair may cause stress concentrations and therefore cracking at other locations in the structure. Drypacking consists in filling a crack with a low w/c ratio mortar and hand-tapping it into place. This technique is appropriate for dormant cracks and for shallow or aesthetic cracks. Post-tensioning consists in drilling holes through the cracks, inserting post-tension rods through the holes and then filling the holes with grout. This repair method will close an open crack and will provide very good resistance. It is important however to provide sufficient anchorage to the bars for risk of causing eccentricities and tensile forces leading to cracking at other locations in the structure. Because of this constraint, this repair method is usually not suitable for the repairs of cracks in most dams. By far the most common repair method for cracks in concrete dams is grout injection (ACI-Committee-224, 1984; United-States-Dept-of-the-Army, 1970).

## **2.3 Injection**

### **2.3.1 Injection Grout Properties**

Grouts have two sets of properties: their rheological properties, before curing, and their hardened properties, once cured. The important rheological properties for injection grouts are their density, stability, granulometry, penetrability, curing time, cohesion, and viscosity. Once cured, the important characteristics are grout density, mechanical resistance, adhesion, chemical resistance, shrinkage, expansion, and resistance to erosion (Mnif, 1997).

#### **2.3.1.1 Stability**

Grout stability is one of the most important characteristics of an injection grout. The stability of the grout reflects the amount of bleeding that occurs in the grout, or the amount of particle sedimentation. A grout is considered stable if the amount of bleeding is less than 5% after 2 hours of being at rest (ASTM, 2003). A stable grout will have little bleeding while an unstable grout will be prone to bleeding and sedimentation, as seen in Figure 2-2. Additionally, the stable grout will be more viscous than the unstable grout. The easiest way to affect the stability in a cement based grout is to modify the w/c ratio (G. Lombardi, 1985b).

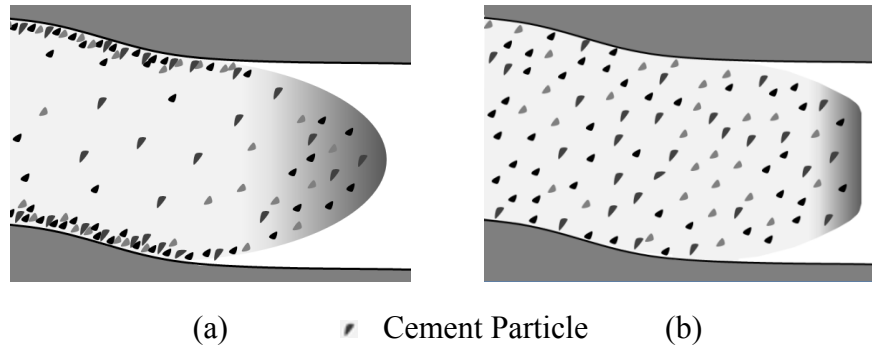


Figure 2-2: (a) Unstable Grout vs. (b) Stable Grout

### 2.3.1.2 W/C Ratio

The w/c ratio is an important variable in cement grouts. A minimum w/c ratio is required to ensure the hydration of all cement particles. As the w/c ratio is increased beyond this point, capillary porosity is increased, leading to weaker cured grout. A low w/c ratio will yield a stable grout having a large density and viscosity before curing and to a cured grout with larger resistances and better cohesion and adhesion. Although a stable grout will yield a cured grout of higher quality, the increased viscosity decreases its injectability. A low w/c ratio will require larger injection pressures to ensure that it propagates through the crack network. To increase injectability, a higher w/c ratio is required (Axelsson, Gustafson, & Fransson, 2009). It has been observed that in cases with an excessive w/c ratio, the cement hydration takes place with individual grains without forming a grout matrix. This results in a fine powder of hydrated cement particles on the bottom surface of the crack. Stability and the w/c ratio of injection grouts are essential in achieving a balance between injectability of the grout and the quality of the cured grout (Giovanni Lombardi, 2007).

Additionally, the w/c ratio has an effect on the strength of the cured grout. As in concrete, a lower w/c ratio leads to a stronger grout. In fact, it was found that in certain grout mixtures, the w/c ratio is the most important factor affecting grout strength (Chen, Ye, & Zhang, 2009).

### 2.3.1.3 Viscosity and Cohesion

The viscosity and cohesion of a grout are determined from flow time, which can be determined by the use of a Marsh cone (ASTM, 2004b). The viscosity of a fluid, measured in Poise, is a

measurement of its internal shear strength. An injection grout with a low viscosity will require smaller injection pressures to deform the fluid and thus to properly penetrate a crack. When a fluid with a large viscosity is being pumped, a much larger force is required to deform the fluid. The cohesion of a fluid is a measurement of the shear force needed to put the fluid in motion. The larger the cohesion of a fluid, the larger the injection pressure required to push the fluid a given distance. Both viscosity and cohesion are closely related properties (Deere & Lombardi, 1985; G. Lombardi, 1985a).

#### **2.3.1.4 Leaching**

When injecting, it is often into a crack filled with water. Because of this, it is important that the grout can resist being washed away by the water and that it does not leach into the water, or mix with the water. The use of a stable grout helps tremendously with the anti-leaching capability of the grout. Studies done by Dumont (1997) found that the use of colloidal admixtures can help greatly with the grouts ability to resist leaching; however, depending on the w/c ratio of the grout, they may not be appropriate since they reduce injectability. It is often necessary to use superplasticizers with the colloidal agents to ensure injectability.

#### **2.3.1.5 Thixotropy**

Thixotropic fluids are fluids that have a relatively large viscosity when they are static, but when agitated, become less viscous. This is an important property of some chemical injection grouts. It can be advantageous because during the injection or pumping of the grout, it has a decreased viscosity that allows for better penetration and injectability. Once the injection process stops, the grout becomes more viscous. This limits the amount of grout that moves out of place or is eroded during the curing process (Mnif, 1997).

#### **2.3.1.6 Maximum Grain Size**

The maximum aggregate size coupled with the injection pressure will determine the minimum crack width that can successfully be injected. The rule of thumb is that the maximum grain size must be at least 3 times smaller than a crack to ensure that no blockage occurs (Axelsson et al., 2009). However it was found by Draganović and Stille (2011) that penetrability can be reduced if too small a grain size is used. This can be attributed to smaller grain sizes having faster hydration

times and larger attraction occurring between particles. This leads to flocculation which can in turn block the flow path.

#### **2.3.1.7 Curing Time**

The set time for injection grouts needs to be well controlled. It is important that the grout does not set before it can properly penetrate the crack being injected. If however the set time is too long, there is a risk of the injection grout being washed out or in cold temperature, freezing (Giovanni Lombardi, 2007).

#### **2.3.1.8 Temperature**

The temperature of the injected medium is of import for grouting. Heat is a necessary part of the chemical reactions that take place during the hydration of cement-based grouts and during the chemical reactions that take place in chemical grouts. To keep grouts warm in cold climates and ensure proper curing, it is possible to use external heat sources and use accelerators to decrease setting time and increase hydration heat (Biggar & Sego, 1990; Zhivoderov, 1993).

### **2.3.2 Types of Grout**

There exists a variety of injection grouts including clay grouts, asphalt grouts, chemical grouts, and cement grouts. New injection materials are always being developed (Argal, Korolev, Kudrin, & Ashikhmen, 2009). An infinite number of different grout properties can be obtained by modifying the components and ratios of these components in a grout mix. For the injection of cracks in concrete dams, the most commonly used are chemical or cement-based grouts (Domone, 1993).

#### **2.3.2.1 Chemical Grouts**

There are wide varieties of chemical grouts available on the market, the most common types being silicate acrylate, lignin, urethane, and epoxy grouts. The most common type of chemical injection grout used for the purpose of crack repair in concrete dams is epoxy-based grouts. Epoxy grouts are typically two separate organic chemicals that are mixed prior to being injected. By modifying the components used, it is possible to obtain epoxy grouts with varying rheological and structural properties so as to be able to obtain the best grout for any given injection. There have been some concerns regarding the proper curing of epoxy grouts at low temperatures since

some degree of heat is required to start the chemical reaction between the two components. However recent developments with epoxy grouts have yielded positive results with the injection repair of cracks at near freezing temperatures (Chertykov & Dzhuraev, 1983; Privileggi, 2012). Another concern with epoxy grouts is that their material properties vary greatly from that of the base material, or mass concrete. For best results in a repair, it is beneficial if the modulus of elasticity of the repair material is roughly equal to that of the base material, but for epoxy, this is usually not the case (Chandra Kishen & Rao, 2007; Morgan, 1996; Rio, Fernandez, & Gonzalo, 2006).

#### **2.3.2.2 Cement Grouts**

By far, the most common injection grouts used for dam repair are cement-based injection grouts. Cement-based grout consists of cement powder mixed with water and different admixtures and additives. Cement is a finely ground powder with a diameter ranging from a few microns to 50  $\mu\text{m}$ . Once water is mixed with the cement, an exothermic chemical reaction called hydration occurs. This reaction leads to the hardening of the grout (Domone, 1993; Saleh, Tremblay, & Desbiens, 1997).

#### **2.3.3 Additives and Admixtures**

There are wide ranges of additives and admixtures that can be incorporated into grout mixes to modify the fluid characteristics and set characteristics of injection grouts. Additives include slag, silica fume, fly-ash, pozzolans, and bentonite to name a few. They are added to the cement powder for the purpose of creating strength gains, enhancing chemical resistance, delaying set time or hydration, increasing cohesion and viscosity, reducing bleeding, and as filler material. Admixtures are added to the grout during the mixing phase and include water-reducing (plasticizers), air entraining, corrosion resisting, set-retarding, and accelerating admixtures (Naudts, Landry, Hooey, & Naudts, 2003).

Accelerators increase the rate at which hydration occurs, they can be useful in cases where important leakages through cracks could disturb the grout before it can properly set. Retarders, on the other hand, are used to slow down the rate of hydration in situations where there is a long delay between mixing the grout and its injection. The simplest way of increasing the injectability of a grout is to increase the w/c ratio. However, as previously discussed, this will decrease the



strength of the hardened grout and decrease the bond between the grout and the injected medium. For this reasons, high-range water reducers or superplasticizers are almost always used for grout injections. Superplasticizers are chemicals that prevent the particles in the grout mix from grouping together, thus decreasing the amount of water required to obtain a stable grout, since clumping and settling of particles is reduced (Naudts et al., 2003).

The effect of the composition of grouts on its rheological behaviour has been widely studied. Many relationships have been developed to predict grout rheology based on the grout mixes (Nguyen, Remond, & Gallias, 2011). Various studies on the effects of particular grout additives have been done. For example it was found by Bremen (1997) that the use of bentonite greatly reduces penetrability of grout mixes and that if penetrability is of import, the use of bentonite should be minimized and the addition of superplasticizers increased. Tests done by Khayat, Yahia, and Sayed (2008) underline the effects of various admixtures and additives on the fluidity, rheology, stability, and compressive strength of grouts. Most notably, it was found that proper dispersion of the agents is important to the final product. The addition of superplasticizers greatly enhances stability and increases grout strength.

### **2.3.4 Injection Methods**

Grout injection is not a definitive science; it is constantly being improved and studied. There exist many different schools of thought on grout injection, such as the classical injection method, the GIN method, and the RODUR method. The basic approach to all of these dam crack injection methods is to drill multiple holes to the crack and to pump an injection grout into the holes in succession. Depending on the method and the crack, different parameters will be measured in real time to determine the progress of the injection, if any injection parameter needs to be modified (grout mix, pressure, etc.), or if the injection should be stopped (Bruce & De Porcellinis, 1989; Giovanni Lombardi, 1998).

A maximum pressure is set for most injections. This maximum is to ensure that the pressure in the crack does not become such that it will cause crack propagation.

The first step with any injection method is to first investigate the cracks. That is to determine the history of the crack, the cause of the crack, whether the crack is active or stable, the flow in the crack, and any other information that may be useful. The next step is to establish an injection

method and its features: the number of injection holes that will be required, injection hole spacing, injection grout properties, injection pressures, real-time measurements, etc. This is why every injection campaign uses a different and unique approach (G. Lombardi, 1997).

As more and more is being understood about grout propagation and grout behaviour, new grouting methods are always being developed, such as the RTCG method by Stille, Gustafson, and Hassler (2012), and the methods discussed by Pronina and Ashikhmen (1996).

#### **2.3.4.1 Classical Injection Method**

This injection method consists of starting the injection process with a grout with a high w/c ratio. As the injection progresses, the w/c ratio of the injection grout is gradually decreased to a specified ideal value. The assumption is that if a low w/c ratio grout is used, the crack will not be filled properly without risk of crack propagation. If, on the other hand, a high w/c ratio grout is used, the quality of the repair will be poor due to the excess water and bleeding. The idea behind this method is that the high w/c ratio grout will be able to penetrate the crack completely. Although the quality of the grout is not ideal, the particles should settle and form a grout layer throughout the entire crack. As the grout w/c ratio is reduced, the quality of the repair should increase. The w/c ratio is gradually decreased until either the injection pressure reaches the pre-specified maximum or until the w/c ratio of the grout reaches its lower limit. This injection method is the most common repair method and has served successfully in countless repair campaigns; however much research has been done suggesting that it is not the most efficient grouting strategy (Giovanni Lombardi, 1998).

#### **2.3.4.2 GIN**

GIN stands for Grout Intensity Number and is represented as a curve on the injection pressure vs. volume curve as seen in Figure 2-3. The GIN method uses a single grout mix for the entire injection. This grout must be stable (w/c ratio between 0.67 and 0.8 by mass), a low-to-medium injection rate must be used, and real-time measurements of pressure and injected volume must be taken. The injection of each individual hole is stopped once the GIN line is intersected on the pressure vs. volume graph (G. Lombardi & Deere, 1993).

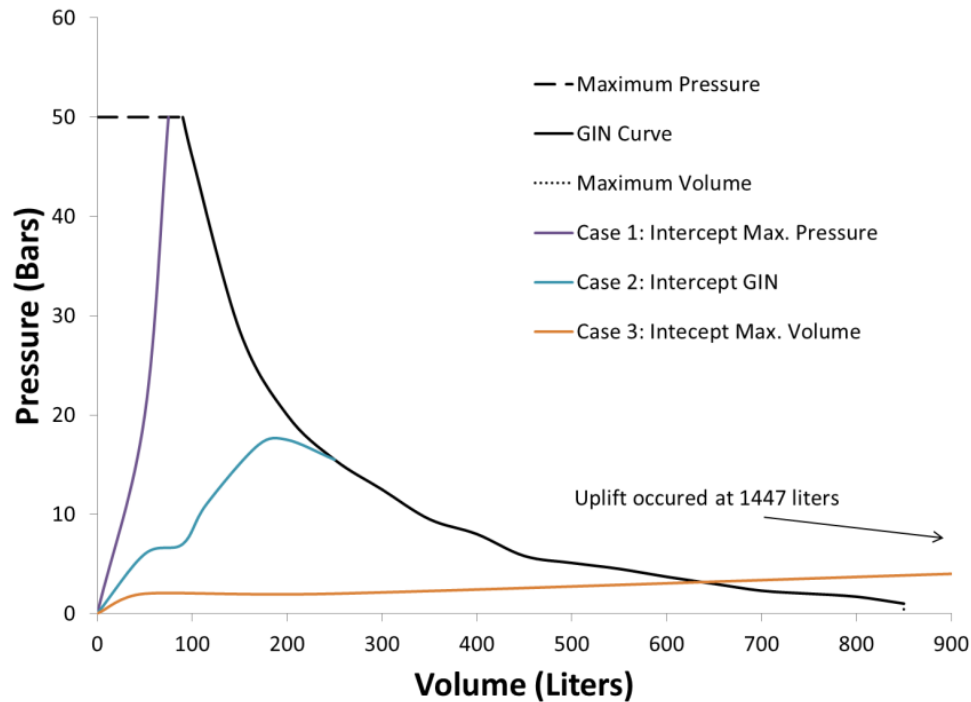


Figure 2-3: Grout Intensity Number and Injection flow paths

### 2.3.4.3 RODUR

The RODUR injection method uses chemical epoxy resin grouts as opposed to cement-based grouts. The grout used for every repair is developed based on the needs of each situation; however, there are some properties that are always desired. The grout must be a true Bingham fluid, must be immiscible in water, and must have a constant and predictable viscosity until set. The RODUR method relies on a single injection at each location. Additionally, crack propagation is not a huge constraint with the RODUR method. This is because the crack is injected in sections so that the entirety of the crack is not subjected to large uplift pressures simultaneously. It is assumed that the portion of the dam not being injected can compensate for the uplift pressure caused at the injection location. It is assumed that the injected pressure decreases very rapidly from the point of injection which further limits the risk of crack propagation. Lastly, if the crack does propagate, it is assumed that it will simultaneously be filled with the grout and repaired (Bruce & De Porcellinis, 1989).

### **2.3.5 Addition Considerations**

Javanmardi and Léger (2005) developed a simplified method considering nonlinear finite element of concrete cracking, hydromechanical coupled analysis, grout state change analysis, and hardened grout in the repair to adequately model the grouting process. It was also shown that the Universal Distinct Element Code software could successfully be used to model the grouting process (UDEEC, 2000).

## **2.4 Repair Case Studies**

### **2.4.1 Isle Maligne Hydroelectric Power Complex**

The Isle Maligne Hydro Electric complex is located in Lac St-Jean, Alma, Quebec, Canada. Local lift joints in the left gravity dam abutment (43 m high by 110 m long) of the dam were repaired by grout injection using the GIN method. The maximum allowable pressure was first selected based on the crack opening, cohesion of the concrete, weight of the concrete, and pre-stressed anchor load. The maximum injection volume was then determined using the maximum pressure, the crack thickness and the concrete cohesion. By multiplying these two numbers (maximum pressure and maximum volume), a GIN value is established. A GIN number was calculated for each section to be injected. The GIN curve (pressure vs. volume) is plotted for each injection point and during the injection, the flow path is plotted on the same graph in real-time. Once it intersects the GIN curve, the grouting is stopped. On Figure 2-3, a sample GIN curve and three (3) observed grouting paths are plotted. Case 1 represents the injection being stopped because the injection pressure reached the specified limit. In this case, no uplift was observed even though the injection pressure was very high. This is due to the fact that the volume of injection grout is small and exerts this pressure over a very small area. Case 2 represents the injection being stopped when the injection path reached the GIN curve. Case 3 represents the case where the crack accepted large volumes of grout with minimal increase in pressure. For this case, the injection was continued past the maximum allowable volume for experimental purposes. It was observed that after exceeding the volume limit, small uplift was observed with no increase to the pressure. At this point, the injection was stopped and the uplift was reversed. This result indicates that there is a risk of uplift even at low pressures. When this pressure is exerted over a large area, uplift can be seen. Except for the case where the injection path was in excess of the

GIN curve (experimental case 3), no uplift was observed (Turcotte, Savard, Lombardi, & Jobin, 1994).

#### **2.4.2 Sayano-Shushenskoe Hydrostation Dam**

The Sayano-Shushenskoe Dam, on the Yenisei River in Khakassia, Russia, is a gravity arch dam with a height of 242 m and length of 1074 m. The water stops and grout curtain proved to be unsuccessful, leading to cracking near the base of the upstream side of the dam and lifting between the dam and bedrock. Once the dam was filled to normal usage levels in 1996, water seepage over a 15 m area near the base of the dam was measured to be 458 liters per second. In 1991, an injection campaign using the classical injection method was undertaken to stop the leakage. Due to the high flow rates in the cracks and the interconnectivity between the cracks, the horizontal drainage holes, cooling pipes, and the investigation bore holes, these repairs proved to be unsuccessful. The injection grout was simply washed out. Many ineffective or failed attempts were made until 1995 when two alternate approaches were attempted. The first using the roflex material (polymer elastic) and the second using the RODUR method. The attempts made with the roflex material failed because the roflex material loses its penetrability at low temperatures and becomes overly viscous. The RODUR injection grout used had high viscosity, good penetrability, low surface tension, and rapid set times at low temperatures. The injections proved successful and completely stopped seepage in the injected section of the dam. Due to this success, an injection campaign to repair the entirety of the seepage was started. Forty injection zones were identified but due to financial constraints, and to the assumption that the compression caused by the injection of some zones would benefit others, 24 injection zones were settled upon. The injection grout used was injected with a pressure varying from 25 to 40 MPa along 15 to 20 m-long injection paths. Due to the length of the path and the viscous nature of the grout, the pressure at the crack mouth was found to vary between 6 MPa and 8 MPa. Extensometers were installed to monitor the movement of the cracks during the injection and an additional crack opening of 2.5 mm was used as a stop criterion for injection. These injections did cause adjacent non-repaired cracks to open further; however, cracks previously repaired did not generally open due to the compression created by their repairs. The repair was successful with only 1% of the seepage remaining in the injected zones (Bryzgalov et al., 1998).

### 2.4.3 Daniel-Johnson Multiple-Arch Dam

Located on the Manicouagan River north of Baie-Comeau in Quebec, Canada, the Daniel-Johnson Dam is the largest multiple arch dam in the world. It has a crest length of 1300 m, a height of 215 m, and a reservoir area of 2000 km<sup>2</sup>, which translates into  $140 \times 10^9$  m<sup>3</sup> of water. The dam consists of 13 cylindrical arches being supported by 14 buttresses (Saleh et al., 2003).

Shortly after its construction which started in 1962 and ended in 1968, the Daniel-Johnson Dam (BDJ) experienced multiple types of cracks and infiltration (Saleh et al., 2002).

Debonding at the base of the dam in most arches was detected due to seepage observed at the base of the structure [Figure 2-4 (b)]. The seepage was stopped by grout injections (Bulota et al., 1991).

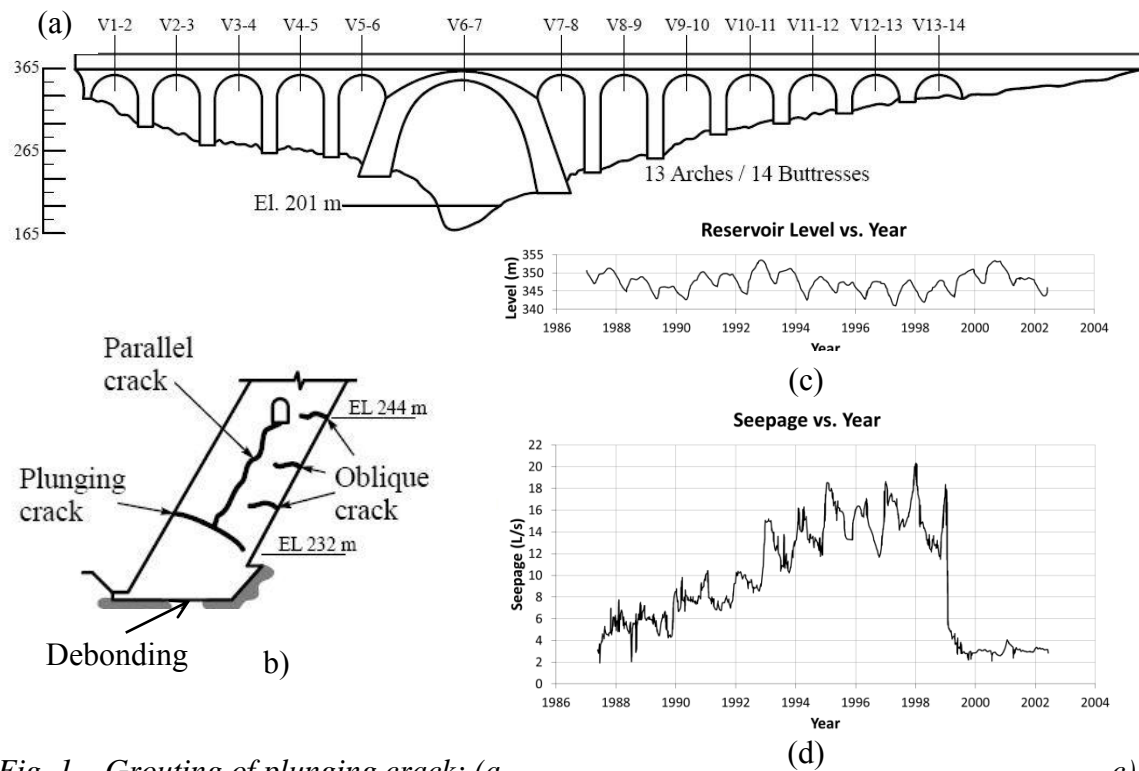


Fig. 1 – Grouting of plunging crack: (a) reservoir level, (d) seepage Arch 5-6.  
 Figure 2-4: Grouting of plunging crack: (a) BDJ dam, (b) typical concrete crack pattern, (c) reservoir level, (d) seepage Arch 5-6

Oblique cracks as seen in Figure 2-4 (b) on the downstream side of the dam were first observed in 1969. These cracks, which are due to thermal stresses, start off being horizontal and form elliptical arcs while moving towards the buttresses. These cracks were generally perpendicular to the downstream face of the dam and on average went to a depth of 35% of the thickness of the dam. Thermal shelters were put in place at the base of the downstream side of the dam to stop the crack propagation (Bulota et al., 1991; Tahmazian et al., 1989).

Plunging cracks, seen in Figure 2-4(b), were caused by a lack of compression in the base of the arches (Larivière, Routhier, Roy, Saleh, & Tremblay, 1999). These plunging cracks initiated in the center of the arches near the upstream foundation of the dam, to then travel horizontally and start diving towards the downstream foundation of the structure (Veltrop et al., 1990).

An injection campaign aimed at repairing these cracks was started in 1969 and ended in 1982 after a moratorium was put on grout injections due to the hydraulic fracturing caused by significant injection pressures using unstable grout with high w/c ratios. After the repairs, the seepage rate increased at a constant rate of roughly 1 l/s per year until 1992, when the seepage rate suddenly increased by 5 l/s in five weeks. A team was put in place to study the problem and in 1997 a grout injection operation was undertaken to repair the plunging crack in arch 5-6 of BDJ using micro fine cement grout [maximum grain size of 12 $\mu$ m (0.472 mils)] (Saleh et al., 2003).

The classical injection method was selected, starting with a grout with a w/c ratio of 1.0 and gradually decreasing it until the stop criteria were met. The stop criteria included a maximum injection pressure of 0.2 MPa above the uplift pressure in the crack and a limited injection area of 100 m<sup>2</sup> (Hydro-Quebec, 2008).

The injection campaign was successful with virtually all of the seepage through the arch having been stopped (Saleh et al., 2003).

## 2.5 Conclusion

Grout injection repairs of dams depend on many factors discussed in this literature review. The properties and composition of the mass concrete being repaired, the properties and composition of the injection grout being used, as well as the specific injection method being used all play an important role in grout injections for dam crack repair. There is still much research and debate

surrounding grouting repairs; however, the material presented in this literature review sets a good foundation for the understanding of the process and sets a starting point for the material presented in Chapter 3.

Although the repairs for BDJ were successful in stopping nearly the entirety of the seepage, it is not known whether this repair actually provides any tensile or shear resistance to the structure. For this reason, it is assumed in numerical models that the tensile resistance for the repaired area is null. As will be presented in Chapter 3 there is reason to believe that this assumption may be overly conservative. The following chapter presents the experimental research done on ascertaining the tensile and shear strengths that the injection for BDJ provided.



## **CHAPTER 3      ARTICLE 1: MECHANICAL RESISTANCE OF CRACKED DAM MASS CONCRETE REPAIRED BY GROUTING: AN EXPERIMENTAL STUDY**

### **3.1 Introduction**

Concrete dams are structures that are prone to cracking. Shrinkage, large temperature gradients, and hydrostatic overload are just some of the causes of cracking in dams. Shortly after its construction, the Daniel Johnson Dam (BDJ) experienced multiple types of cracks including plunging cracks which were caused by a lack of compression in the base of the arches.<sup>1,2</sup> These plunging cracks initiated in the center of the arches near the upstream foundation of the dam, then travel horizontally and start to dive towards the downstream foundation of the structure (Figure 3-1 a). To minimize water infiltration and leakage as well as to improve structural integrity by eliminating uplift pressures, these crack needed to be repaired.

There are various methods of repair techniques ranging from post-tensioning to injections following different procedures and using different materials. In the case of BDJ and for similar types of cracks, the most common repair method is grout injection.<sup>3</sup>

An injection campaign aimed at repairing these cracks was started in 1969 and ended in 1982 after a moratorium was put on grout injections due to the hydraulic fracturing caused by significant injection pressure using unstable grout with high water cement (w/c) ratio.<sup>4</sup> Since, many repair products including epoxy based grouts, and micro fine cement grouts have been studied and tested.<sup>5,6,7,8</sup> In 1997 a grout injection operation was undertaken to repair the plunging crack in arch 5-6 of BDJ using stable micro fine cement grout [maximum grain size of 12 $\mu$ m (0.472 mils)]. From Figure 3-1, after the injection operation, the total water leakage from arch 5-6 and buttresses decreased from roughly 19 L/s (1159.5 in<sup>3</sup>/s) to 3 L/s (183.1 in<sup>3</sup>/s). The repair is important not only to decrease leakage but also to remove uplift pressures that the water in the cracks creates.<sup>1,4</sup>

Since the injection, as can be seen from Figure 3-1, the water level in the reservoir has increased to above pre-repair levels without having a noticeable effect on water leakage. These results suggest that the repair increases the ability of the crack mouth in BDJ to sustain tensile stresses post-injection. In the finite element models used to assess the initiation and propagation of

grouted crack it is most often assumed that there is no gain in mechanical strength because little data exists on the strength a repair may provide in mass concrete.<sup>9</sup>

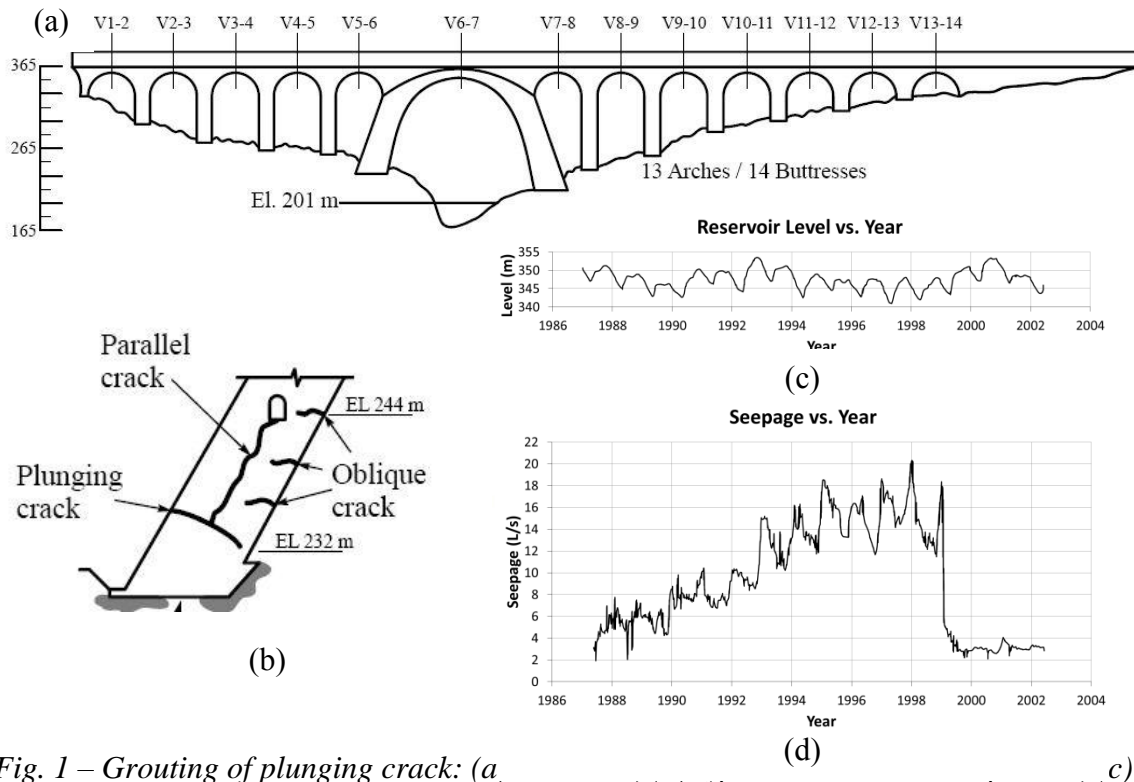


Fig. 1 – Grouting of plunging crack: (a) BDJ dam, (b) typical concrete crack pattern, (c) reservoir level, (d) seepage Arch 5-6

Figure 3-1: Grouting of plunging crack: (a) BDJ dam, (b) typical concrete crack pattern, (c) reservoir level, (d) seepage Arch 5-6

Injection grout research is well documented in terms of rheology, composition, and injectability.<sup>10,11</sup> There have been some studies done on the tensile strength of mass concrete and on cold jointed concrete, however the strength of a repaired section of mass concrete has yet to be studied.<sup>12,13,14</sup> In the work presented here, the tensile and shear resistance of mass concrete and repaired mass concrete was investigated experimentally following a modified ASTM C78 test procedure and a shear test procedure.<sup>15</sup> Results from virgin specimens, repaired with an injection grout with a water cement ratio of 1.0 (Grout I) and of 0.5 (Grout II), were compared. This research provides experimental failure behaviour and resistances of mass concrete and the related grouted cracks under flexural loading and shear loading.

## **3.2 Research Significance**

Many studies have been undertaken on the repairs of dams as well as on various different injection grouts and repair methods, however there is little literature or experimental research on the mechanical strength of repaired sections of concrete, especially mass concrete. This experimental study is useful in determining the modulus of rupture and shear strength of repaired mass concrete while not having to account for the scaling factor of the aggregate size. This study also provides valuable experimental data to assign mechanical strength in numerical models of repaired dams including grouted cracks.

## **3.3 Experimental Investigation**

### **3.3.1 Mass Concrete Mix and Related Properties**

The initial BDJ concrete mix used 150 mm (6 in.) max size aggregate. To properly account for the rugosity of the large aggregates, but given the constraints of the laboratory, maximum aggregates of 100 mm (4 in.) were selected for the experimental concrete mix. All specimens tested were from the same concrete mix; three batches were needed to pour all six prismatic beam specimens used [400 x 400 x 1250 mm (16 x 16 x 49.2 in.)]. The maximum aggregate size was 100 mm (4 in.) or 2/3 the max aggregate used for BDJ. Due to the large maximum aggregate size, the minimum dimension of a given specimen could not be smaller than 300 mm (12 in.);<sup>16</sup> 400 mm (16 in.) was chosen to be conservative. The following are the components of the mix which can be found in Table 3-1: General Use Portland cement (Low Heat cement was not used because it has little effect on the strength and would increase cure time), superplasticizer (to increase workability), entrained air, well graded siliceous river sand, and well graded limestone aggregate. The mix was developed by modifying the original 1967-68 mix of BDJ while keeping similar granulometry and composition and to have a compressive strength of 30 MPa (4.35 ksi), roughly the initial compressive strength of BDJ, while making the concrete workable.<sup>7</sup>

Table 3-1: Mass Concrete Mixes

1967-68 BDJ Mix			Final Experimental Concrete Mix		
Material	1000 L		Material	1000 L	
Cement**	234	kg	Cement	270	kg
Large Sand	364	kg	Sand	675	kg
Fine Sand	363	kg			
Aggregate 20-10	148	kg	Aggregate 5-10	305	kg
Aggregate 38-20	231	kg	Aggregate 10-20	220	kg
Aggregate 75-38	445	kg	Aggregate 20-40	345	kg
Aggregate 150-75	534	kg	Aggregate 50-100	450	kg
Water***	113	kg	Water	143	kg
			Entrained air	770	ml
Entrained air	0.3	kg	Superplasticizer	3090/2730*	ml

\* Batch 2 and 3, \*\* LH, \*\*\*Frozen (Ice)

Note: 1 kg = 2.20lb, 1L = 61.02in<sup>3</sup>, 1ml = 0.06102in<sup>3</sup>

Three cylinder specimens, seen in Figure 3-2, of 400 mm (16 in.) diameter and 800 mm (32 in.) in height, one from each batch of concrete, were poured into cardboard tubes. A modified version of ASTM C469 (to account for the larger specimens) was used to determine the compressive strength, modulus of elasticity, and Poisson's ratio of the concrete.<sup>17</sup> The size effect for the results of the compressive strength are negligible.<sup>18</sup>



Figure 3-2: Mass concrete cylindrical specimen (400mm x 800mm)

### 3.3.2 Grout Mixes and Related Properties

When repairing a dam, a grout with a low w/c ratio is desired because it will bond more strongly with the parent material and will have better mechanical strength.<sup>19</sup> In practice this is often not possible, due to the irregular shape and varying thicknesses of cracks; if a grout is too viscous it will not properly fill the entire crack under low pressures. For these reasons, a higher water cement ratio is often used for grout injection.<sup>9</sup> The latest approach which was used in the repair of BDJ was to start the injection with a water cement ratio of 1.0 and gradually decrease it until no longer possible, ending the injection with a water cement ratio ranging anywhere from 1.0 to 0.4.<sup>20</sup>

In this study, two grout mixes, seen in Table 3-2, were used for the injections; either a grout mix with a water cement ratio of 1.0 (Grout I), or a grout mix with a water cement ratio of 0.5 (Grout II). Both mixes used micro fine cement [maximum grain size 12 $\mu$ m (0.472 mils)] and a superplasticizer. The grout mixes used are equivalent to the mixes used in the repair of the BDJ.<sup>20</sup> The rheological tests performed on each grout mix were bleeding, according to ASTM C940;<sup>21</sup> viscosity, according to ASTM D6910;<sup>22</sup> set time, using a thermocouple; and density. At least twelve 25.4mm (1 in.) cylindrical specimens and nine 50.8 mm (2 in.) cylindrical specimens, that meet the specifications of ASTM C 579 and ASTM C 496 respectively, were tested with each injection.<sup>23,24</sup> For the first injection of both specimens A and B (Table 3) no 50.8mm (2 in.) cylindrical specimens were poured for compressive strength tests. Cylindrical specimens of 25.4mm (1 in.) diameter were tested in accordance with ASTM C 579.<sup>23</sup> Cylindrical specimens of 50.8 mm (2 in.) were tested in compression following ASTM C 39 or in indirect tension following ASTM C 496.<sup>24</sup>

Table 3-2: Grout Mixes

Ingredients	(I) W/C = 1.0		(II) W/C = 0.5	
	V	m	V	m
	[L]	[kg]	[L]	[kg]
Micro-fine cement	4.21	12.39	4.25	12.5
Water	12.14	12.14	6	6
Superplasticizer	0.25	-	0.25	-
Total	16.6		10.5	

Note: 1 L = 61.0237 in<sup>3</sup>; 1 kg = 2.20462 lb.

### 3.3.3 Beam Specimens

Six 400 x 400 x 1250 mm (16 x 16 x 49.2 in.) unreinforced mass concrete specimens were cast (Table 3-3). Each specimen had a notch around its center which was 25 mm (1 in.) deep and 19mm (3/4 in.) wide. This notch was to ensure that the crack initiated in a predicted location and to favour grout penetration for the repair. The specimens were fitted with 10M rebar outside of the crack zone for transportation purposes. To attach the support frames to the specimens, anchors were mounted to the cured specimens. Bolts were then used to attach the support frame. The frames seen in Figure 3-3 consists of two „U“ shaped steel assemblages that are at either end of the specimen and are attached by means of four 25 mm (1 in.) steel rods. In cases in which the specimen was to be repaired, a hole was drilled to the center of the specimen prior to the test to create an exit point for the grout during injection. The drilled holes were capped with an exit valve so that pressure could be controlled.

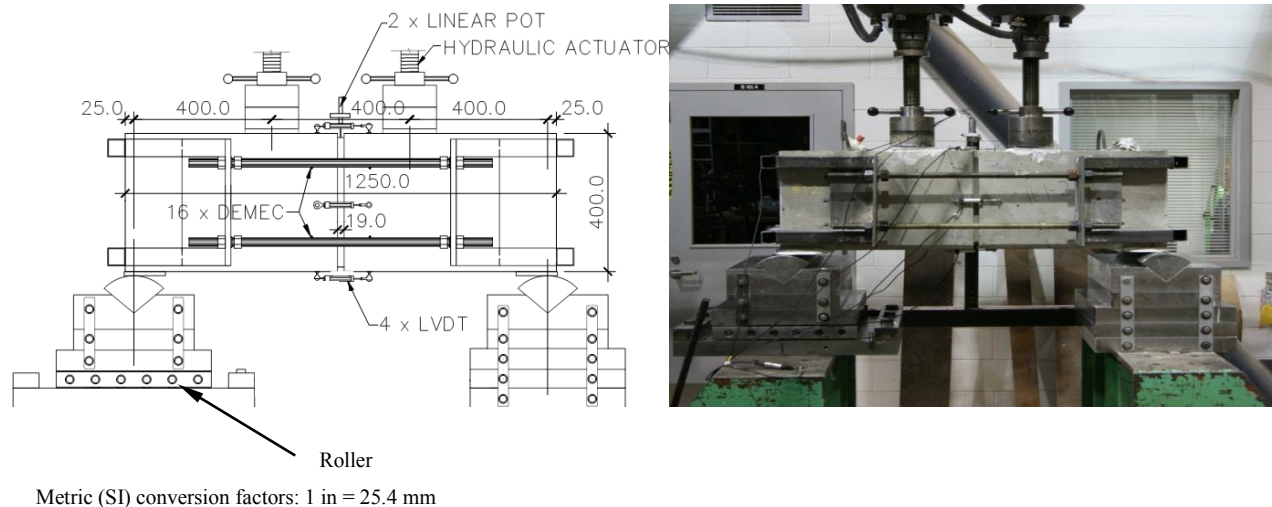


Figure 3-3: Modified Modulus of Rupture – ASTM C 78

### 3.3.4 Testing Program

The Testing program, summarized in Table 3-3, consists of the modulus of rupture tests, injections, and shear tests.

Table 3-3: Specimens and Test Order

Specimens	A	B	C	D	E	F
Modulus of Rupture	x	x	x	x	x	x
Initial Repair W/C ratio:	1	0.5	1	0.5	-	-
Modulus of Rupture	x	x	-	-	-	-
Second Repair W/C ratio:	1	0.5	-	-	-	-
Modulus of Rupture	x	x	-	-	-	-
Third Repair W/C ratio:	1	0.5	-	-	-	-
Shear Test	x	x	x	x	-	-
Batch	1	3	2	1	-	-

### 3.3.5 Modified Modulus of Rupture ASTM C78

To determine the modulus of rupture of the concrete, all six specimens were first tested using a variation of ASTM C78, Standard Test Method for Flexural Strength of Concrete. The two differences were the specimen size and the notched center. The Specimens were larger than the size prescribed by the standard due to the large aggregates. ASTM C78 does not call for a notched specimen. The geometric proportions prescribed by the standard were followed.<sup>15</sup> To apply the load, two 245 kN (55 000 lb) hydraulic jacks were used. As shown on Figure 3-3, a spacing of 400 mm (16 in.), 1/3 the total length, was set between any given support and the nearest load and between the two loads. The total span between the two supports was 1200 mm (47 ¼ in.). Both ends of the specimens were fitted with a steel frame. The two frames were connected to each other by four 25.4 mm (1 in.) steel rods fitted with four bolts each. The frame served two purposes: ensuring that the two ends, upon fracture, would not fall; and to allow the two pieces to be re-aligned with a specific crack opening. The vertical displacement at mid-span was measured with two linear variable displacement transducers (LVDTs). The horizontal deflection at the center of the specimen was measured with four Linear Potentiometers (LPs). The force applied to the specimen was measured by a load cell located in the control system of the actuators. Specimens A and B were repaired by grout injection and retested 28 days later (Table 3-3). This was repeated twice. They were subsequently tested in shear. Specimens C and D were repaired by grout injection and then tested in shear. Specimens E and F were not repaired to allow examination of the failure plane.

### 3.3.6 Grouting Repair

In the repair of BDJ, the injection pressure needs to be superior to the water pressure found at the crack mouth to ensure that the water in the crack is flushed and replaced by the injection grout. It is important that the injection pressure not be too high because this increase in pressure inside the dam could cause crack propagation. It was found that 0.2 MPa (30 psi) above the water pressure found at the crack mouth was an appropriate injection pressure to adequately flush the water while not propagating the crack.<sup>4</sup> In the case of the injection of BDJ, the concrete is completely saturated.<sup>20</sup>

The temperature of the concrete injection in BDJ was roughly 4 °C (39.2 °F). The injections for the experimental procedure were done at room temperature, roughly 20 °C (68 °F).<sup>4</sup> The effects of the temperature were not taken into consideration.



Figure 3-4: Injection and Injection Frame

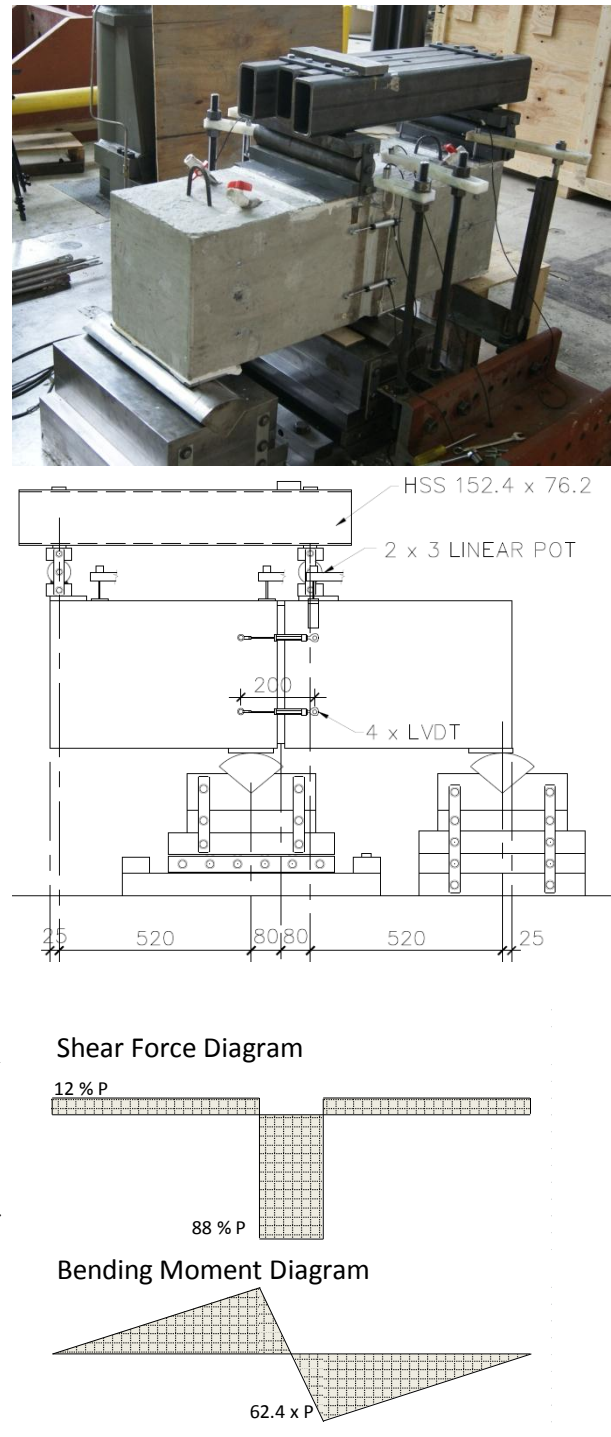
The specimens were mounted with a support frame as seen in Figure 3-4. Upon failure of the specimen the crack between the two specimen halves was set to 2 mm (78.74 mil); this opening was selected so as not to impede the injection grout and to insure the best repair possible. This range of opening is representative of some of the openings at the crack mouth of BDJ. This was done with the help of 8 pairs of DEMEC points and by adjusting bolts on the 4 rods. The injection frame was installed on the specimens (A,B,C, and D) to allow the fracture to be repaired. The frame consisted of four 100 x 420 x 12 mm (4 x 16 x 1/2 in.) piece of pure gum that were held against the four sides of the specimen by steel plates. The plates were compressed onto the specimen by bolts attached to a steel frame that is installed around the specimen to seal the



specimen perimeter. Water was flushed through the crack with a manual pump to clean out any debris or dust. The water was then pressurized to 0.2 MPa (30 psi) to test the seal and ensure water tightness. The pressure was maintained for at least 24 hours to saturate the concrete as would be the case for BDJ and so that the concrete would not absorb water from the grout. A grout mixture, which can be found in Table 3-2, was then flushed through the specimen to ensure that the water was entirely evacuated from the crack. Once all the water was flushed and grout filled the entirety of the crack, the exit valve was closed. The pressure was elevated to and maintained at 0.2 MPa (30 psi) until the grout set. The injection frame was removed after 7 days. After removing the injection frame, the crack width was measured with the DEMEC points. Due to the pressure in the crack during the injections, the crack width has a tendency to open so that the layer of repair grout is in fact found to be larger than 2 mm (78.74 mil), being closer to 3 mm (118.1 mil). This was repeated twice more for specimens A and B (Table 3-3).

### 3.3.7 Shear Test

A shear test, modified from that proposed by Bazant et al.<sup>26</sup>, was performed on the 4 repaired specimens, A, B, C, and D. The modifications to the test were the use of larger specimens and a smaller notched center. Figure 3-5 (a) shows that



Metric (SI) conversion factors: 1 in = 25.4 mm

Figure 3-5: Shear Test Setup: (a) Test Setup; (b) Shear Force and Bending Moment Diagram

the specimens were placed on two supports; the first support being 25 mm (1 in.) from the beam end and the second 680 mm (27-3/4 in.) from the first support. A single 12 MN (1350 ton-force) actuator was used to apply the load at the center of the specimen to a HSS transfer beam. By geometry, this beam in turn applied a load of 12% and 88% of the total applied load to the specimen at 25 mm (1 in.) from the hanging end and 680 mm (27-3/4 in.) away from this point. The horizontal displacement was measured using four LPs with a gauge length of 200 mm (8 in.). The vertical displacement was measured by 6 LVDTs; 2 above the centrally applied load, 2 above the central reaction and 2 at the overhang.

### 3.4 Experimental Results and Discussion

#### 3.4.1 Mass Concrete Mix and Related Properties

The properties of the mass concrete developed, found in Table 3-4 and Table 3-5, were similar to BDJ concrete. The compressive resistance of the concrete used for BDJ was targeted to be 30 MPa (4.35 ksi) (although now it is 40 MPa (5.8 ksi)). The average compressive resistance of the experimental concrete was 28 MPa (4 ksi). The elastic modulus and Poisson's ratio from batch one was not available due to an instrumentation problem. The average elastic modulus and Poisson ratio were, omitting results for batch one, 33.4 GPa (4844 ksi) and 0.12 respectively which again, is representative of the same properties for BDJ concrete.<sup>7</sup>

Table 3-4: Concrete Rheology

Batch #	Slump/Spread [mm]	Temperature [°C]	Air [%]	Density [kg/m <sup>3</sup> ]
1	250 / 545	25	4,2	2339,5
2	190 / 365	26.2	4,7	2288,4
3	60 / 205	26	6,8	2232,1
Average	167 / 372	25.7	5,2	2286,7

Note: 1 mm = 0.0394 in; 1 °C x 9/5 + 32 = 1 °F; 1kg = 2.20462 lb; 1 m<sup>3</sup> = 35.3147 ft<sup>3</sup>

Table 3-5: Concrete Properties

Batch #	Resistance f' <sub>c</sub> [MPa]	Modulus E [GPa]	Poisson v [m/m]
1	29.3	N/A	N/A
2	28.0	33.7	0.115
3	26.7	33.0	0.132
Average	28.0	33.4	0.124

Note: 1 m = 39.37 in; 1 MPa = 145.0377 psi; 1 GPa = 145.0377 ksi

### 3.4.2 Grout Mixes and Related Properties

Although the grout had a very large compressive resistance, the material was very brittle, delicate, and friable after air drying. One in three of the test cylinders were broken while being removed from their moulds or while being manipulated. The failure mode for the compressive tests was very brittle or explosive failure; this is true for both the 25.4 mm (1 in.) and the 50.8 mm (2 in.) cylinders. In the case of the Brazilian splitting test, the failure was observed to be two clean fractures down the center of the specimen leaving a small intact band in the center. This was expected as there were no aggregate. Based on the bleeding test, Grout I was considered unstable with significant cement particle settlement as indicated while Grout II is considered stable with cement particle remaining in suspension in the mix. From Table 3-6, the grout rheology and strength were equivalent to the grout used in BDJ and the results given by the grout manufacturer.<sup>20,27</sup>

Table 3-6: Grout Properties and Rheology

	Bleeding [%]	Flow Time [sec]	Density [Relat.]	Set Time [h]	f' <sub>c</sub> [MPa]	Brazilian [MPa]	f' <sub>c</sub> 2" cylinder [MPa]
Grout I	3.75	32.27	1.51	8.0	49.09	2.43	43.51
Grout I	4.38	31.93	1.49	6.5	24.43	1.81	-
Grout I	3.00	29.47	1.49	7.0	45.71	2.45	36.93
Grout I	5.13	31.13	1.49	7.0	33.33	1.52	40.49
Grout II	0.13	150.7	1.78	8.0	37.70	3.96	69.09
Grout II	0.63	262.0	1.68	7.0	53.96	4.04	-
Grout II	0.13	285.6	1.73	9.0	69.01	3.03	58.25
Grout II	0.00	256.1	1.78	7.0	37.69	3.41	30.49
Avg Grout I	4.06	31.20	1.50	7.1	38.14	2.05	40.31
Avg Grout II	0.22	238.6	1.74	7.8	49.59	3.61	52.61

Note: 1 MPa = 145.0377 psi

### 3.4.3 Modulus of Rupture

The failure of both virgin and repaired specimens was brittle. The failure plane of virgin specimens, Figure 3-6, stayed in the concrete matrix and avoided most large aggregates, leaving them intact and protruding from the failure plane. The failure plane of repaired specimens followed the same path as for virgin specimens along the interface between the concrete and the injection grout. The failure plane propagated from one concrete surface through the grout to the other concrete surface depending on the positioning of the aggregate. The modulus of rupture of a virgin specimen, found in Table 3-7 and Figure 3-7, was 2.79 MPa, which is, 10% that of the compressive strength of the concrete.<sup>12</sup> After being repaired, the modulus of rupture was significantly reduced. For injection Grout I and Grout II, it was 0.55 MPa (80 ksi) and 0.95 MPa (138 ksi) respectively as seen in Table 3-7 and Figure 3-8. Multiple repairs had no noticeable effect on the modulus of rupture. The modulus of rupture of the repaired specimens was not reflective of the strength of the virgin concrete or the strength of the repair grout. The modulus of rupture exhibited distinct properties as a hybrid material being tributary of the adhesive strength between the grout and the concrete surface made of cement paste and aggregates. The increased modulus of rupture for a specimen repaired with a grout with a favourable or lower w/c ratio is not due to the grout being stronger, but due to the bond formed between the grout and the concrete. A lower water cement ratio increased bleeding and decreased density of grout as seen in Table 3-6. This in turn decreased the bond strength between the parent material and the injection grout.



Figure 3-6: Modulus of Rupture Failure Plane (Specimen E)

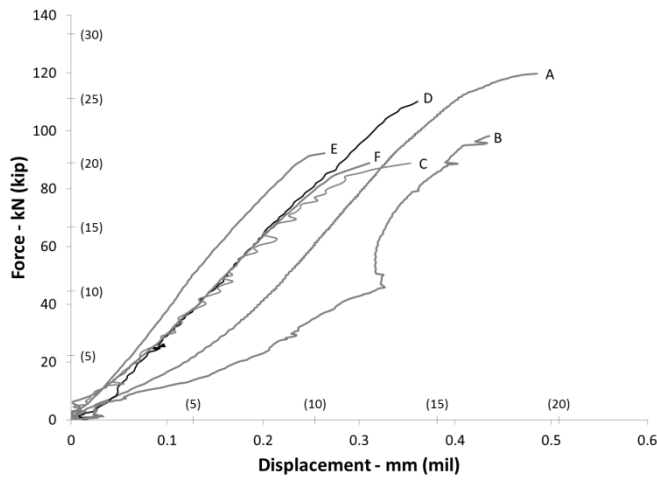


Figure 3-7: Force vs. Displacement of Virgin Specimens (A to F)

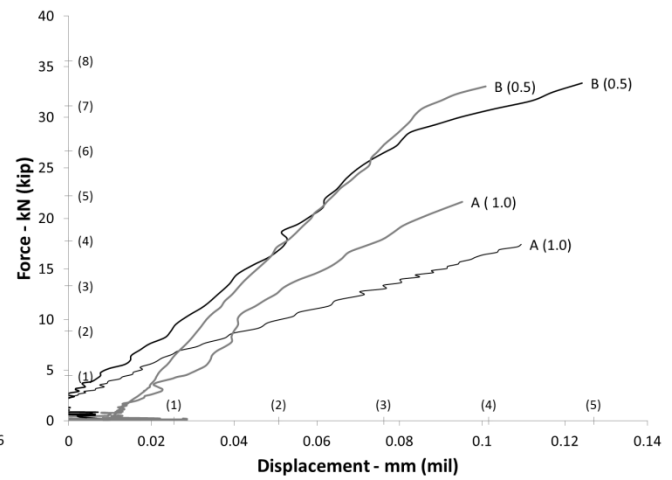


Figure 3-8: Force vs. Displacement of Repaired Specimens (A (grout w/c) and B (grout w/c))

Table 3-7: Modulus of Rupture Test Results

Specimen	Test #	W/C	Max Force [kN]	Max Avg. Deflection [mm]	Max Stress [MPa]
A	1	-	119.8	0.487	3.35
A	2	1	17.4	0.057	0.49
A	3	1	21.6	0.056	0.61
B	1	-	98.2	0.432	2.75
B	2	0.5	33.4	0.120	0.93
B	3	0.5	33.1	0.096	0.93
C	1	-	88.8	0.355	2.49
D	1	-	110.2	0.356	3.08
E	1	-	92.3	0.223	2.58
F	1	-	88.9	0.300	2.49
Average for	1	-	100	0.359	2.79
Average for	2	-	25	0.088	0.71
Average for	3	-	27	0.076	0.77
Average for	-	0.5	33	0.108	0.93
Average for	-	1	20	0.056	0.55

Note: 1 kN = 224.8089 lbf; 1 mm = 39.3701 mil in; 1 MPa = 145.0377 psi

### 3.4.4 Shear Strength

The shear failure in all cases was brittle. The failure plane, seen in Figure 3-9, and shear resistance, seen in Table 3-8, are dependent on two factors: the crack width and the repair grout w/c ratio.

Table 3-8: Shear Test Results

Specimen #	W/C	Vr [kN]	$\tau_{(Vr)}$ [MPa]	Number of Repairs	Crack Width [mm]
A	1	70	0.57	3	9.5
B	0.5	251	2.05	3	8.3
C	1	351	2.87	1	3.1
D	0.5	457	3.73	1	2.5

Note: 1 kN = 224.8089 lbf; 1 mm = 39.3701 mil in; 1 MPa = 145.0377 psi

In the case of a thin width of grout and a low w/c ratio, two failure planes developed, the first has a tendency to go from the central applied load to the central reaction, forming a new crack through the un-cracked concrete which travels through both aggregates and the matrix [Figure 3-9 (b)]. This type of failure does not tend to circumvent the aggregates but shears a lot of them. The second failure plane observed traveled, as seen in the modulus of rupture test, at the concrete-grout interface [Figure 3-9 (a)]. A thin layer of low w/c ratio repair grout leads to a stronger repair.

In the case of a wide width of grout and a high w/c ratio, the shear strength of the repair decreases. This also leads to only a single failure plane forming in the initial crack at the concrete-grout interface as with the modulus of rupture test. It propagates through the interface moving from one concrete surface to the other depending on the aggregate placement [Figure 3-9 (a)]. A high w/c ratio and large crack width leads to the lowest shear strength.

When a large crack width is coupled with a low w/c ratio grout or a thin crack is coupled with a high w/c ratio grout, the strength is found to be somewhere in between the previously mentioned „best“ case and „worst“ case scenarios. Additionally, the failure plane observed is a combination of the two. As was observed in the previous two cases, the concrete-grout interface failure plane occurs, however, the inclined failure plane is also partially present. In this case, some cracking is observed on this failure plane but not in its entirety.

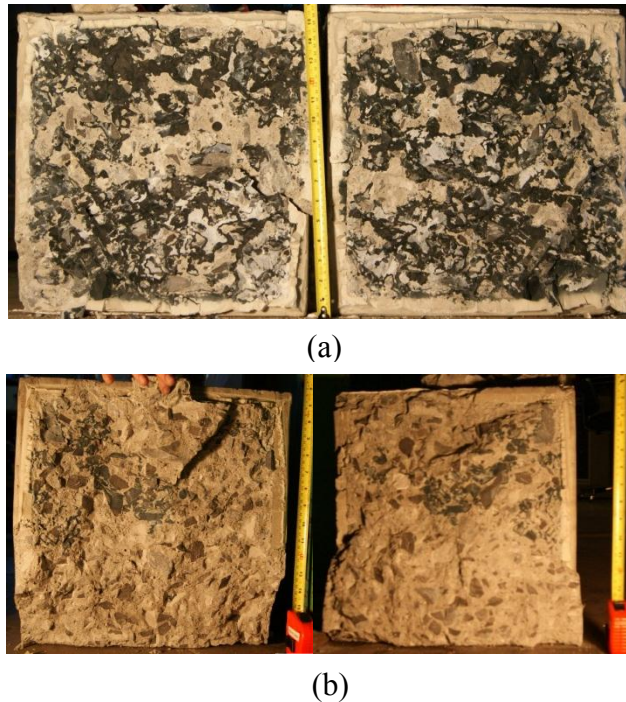


Figure 3-9: Shear Failure Plane: (a) vertical failure plane – Specimen B; (b) inclined failure

With a thin grout layer, the weakest section of the repaired specimen, the grout concrete interface, is only solicited on a very small section near the middle. As this layer gets wider, the area of grout being solicited increases, decreasing the maximum resistance. Additionally, as the grout layer widens, there is an increased influence from the moment on the failure mechanism as can be seen from Figure 3-5 (b).

When comparing specimens with similar grout thicknesses (A-B and C-D) the specimen repaired with the lower w/c ratio had higher shear strength. Again, this is due to the adherence between the grout and the concrete and not the actual strength of the grout. In the case of a thin grout layer, the effect of the grout w/c ratio is less noticeable due to the fact that only a small portion of the grout is being solicited. As this layer thickens, the grout w/c ratio becomes more important and more influential on the shear resistance of the specimen.

### 3.5 Summary and Conclusions

The purpose of this paper was to investigate the modulus of rupture and shear strength of repaired dam mass concrete. The experimental program included a modified 4 point modulus of rupture

test, a shear test, and a pressurized grout-injection repair protocol performed on six 400 x 400 x 1250 mm (16 x 16 x 49.2 in.) mass concrete specimens. Based on the results of this experimental investigation, the following conclusions are drawn:

1. Concrete Mix

A concrete mix with similar properties to the BDJ mass concrete with maximum aggregate size of 100 mm (4 in.) was developed. The concrete mix developed was more workable than the original BDJ mix so that it could be used in laboratory settings.

2. Grout Mix

Injection grouts with a water cement ratio by weight of 1.0 and 0.5, the range used for the injection BDJ, were successfully used to repair mass concrete specimens. The grout mix was virtually identical to the grout mix used in the injection of BDJ and the grout properties tested were also the same.<sup>20</sup>

3. Injection

An injection system able to maintain pressure was successfully developed and implemented to sustain the injected grout at a pressure equal to or above 200 kPa (30 psi).

4. Modulus of Rupture

Failure Mechanism

A brittle failure was observed in the case of both the virgin specimens and repaired specimens. In the case of the virgin specimens, the crack propagated itself through the concrete matrix and avoided aggregates, preferring to circumvent them instead. In the case of the repaired specimens, either single or multiple repairs, the crack propagated itself in the initial crack at the interface between the concrete and the grout. It did not stay on one concrete surface; it travelled through the grout to move from one concrete surface to the other depending on the arrangement of the aggregates.

Strength

The modulus of rupture of the virgin specimens was equal on average to 2.8 MPa (406 psi) or 10% of the concrete compressive strength. The modulus of rupture of the repaired specimens on average, when repaired with Grout I (w/c = 1.0) and Grout II (w/c = 0.5) is equal to 0.55 MPa (80



ksi) and 0.95 MPa (138 psi) respectively. The quality of the grout has an effect on the strength of the repair; however, the hybrid material's modulus of rupture is smaller than that of either the concrete or the grout and is tributary of the adhesive properties between the grout and the hardened cement paste and aggregates along the crack surfaces.

## 5. Shear Test

### Failure Mechanism

The failure mechanism was always brittle, however the failure plane varied depending on the thickness of the grout and w/c ratio of the repair grout. With a thick layer of grout and high w/c ratio repair grout, the crack occurred on the same failure plane as with the modulus of rupture test. It traveled through the concrete-grout interface around aggregates moving from one concrete surface to the other depending on the aggregate placement. In the case of a thin layer of grout and a low w/c ratio repair grout two failure planes occurred; one being the same as with the thick grout layer while the other travelled from the point of application of the load towards the reaction. This new failure plane that was created traveled through, and sheared some aggregates. When a combination of these two factors was used, the failure plane observed was the concrete-grout interface failure plane as well as partial cracking on the new oblique failure plane.

### Strength

The shear resistance observed ranged from 3.73 MPa (541 psi) to 0.57 MPa (83 psi). The quality of the grout has an effect on the shear resistance; specimens repaired with Grout II had a better shear resistance than those repaired with Grout I. The effect of the grout layer thickness was much more important. In cases where the grout layer is thicker, a much lower strength was observed.

## 6. Structural Significance of the Results

Grouted mass concrete cracks could mobilize 1 to 0.5 MPa (145 psi to 72.5 psi) and 3.73 to 0.57 MPa (541 psi to 82.7 psi) in tension and shear respectively. This is significant for the prevention of further cracking during the service life of dams given an increased applied loading. The tests were performed on fresh cracks under controlled laboratory conditions. This may not reflect the reality in the field where cracks may have been leaking for years leading to potential erosion,

calcite formation, and build-up of sediments. Caution should be used when extrapolating these results to actual structures.

## 7. Recommendations

These results show that the no-tension assumption, that is currently in use for the modeling of repaired crack section, is conservative. In fact the experimental procedure undertaken shows that the grouting repair provides a structurally significant tensile and shear strength. This means that the models currently used could be improved to account for this increase in strength provided by the repair. This is conditional to in situ quality control of the grouting work. This would allow for the dam reservoir to be increased by a certain amount without crack re opening.

Further research is being considered to assess the effects of a normal force in the mobilized shear strength to establish a Mohr-Coulomb type of failure envelope and to consider more complex stress state representative of each dam in service while cracking and assessing the strength of repaired specimens.

## 3.6 Acknowledgments

The authors would like to thank the National Science and Engineering Research Council of Canada (NSERC), and the Quebec Funds for Research on New Technologies (FQRNT) for financing this research work, the Hydro-Quebec Engineers who provided information on crack grouting done on the Daniel Johnson Dam, Holcim for providing the injection grout, and M.-A Tessier for his work on the experimentations.

### 3.7 References

1. Larivière, R.; Routhier, L.; Roy, V.; Saleh, K.; Tremblay, S., "Grouting of the cracks in the arch 5-6 of Daniel-Johnson Dam," Management of dams for the next millennium, Canadian Dam Association Annual Conference, Sudbury, Canada, Oct. 1999, pp. 189-195.
2. Veltrop, J. A.; Yeh, C.-H.; and Paul, W. J., "Evaluation of cracks in a multiple arch dam," Dam Engineering, 1990, V. 1, No. 5, pp. 5-12
3. Lapointe, R., "Contributions to the study of grout injection in cracked concrete," McGill University Thesis, Montreal, Quebec, Canada, 1997. 125 pp. (in French)
4. Saleh, K.; Tremblay, S.; Lizotte, M.; Larivière, R.; Roy, V.; and Routhier, L., "Crack repair in concrete dams: identifying effective methods and materials," Hydro Review, 2002, V. 21, No. 5, pp. 40-49.
5. Turcotte, L.; Savard, B.; Lombardi, G.; and Jobin, H. "The use of stable grout and GIN technique in grouting for dam rehabilitation," Canadian Dam Safety Association (CDSA) Conference, Winnipeg, Manitoba, Canada, 1994, BiTech Publishers, pp. 137-162.
6. Tahmazian, B.; Yeh, C.-H.; and Paul, W. J., "Thermal cracking and arch action in Daniel Johnson dam." International Commission On Large Dams, International Symposium on Analytical Evaluation of Dam Related Safety Problems, Copenhagen, 1989, V. 1, pp. 235-244.
7. Bulota, G.; Im, O.; and Larivière, R., "The Daniel-Johnson dam : a premature ageing," International Commission on Large Dams, 17<sup>th</sup> Congress, Vienna, 1991, V. 2, pp. 187-209. (in French)
8. Saleh, K.; and Dumond, C., "Study on micro-fin cement based injection grouts," Rapport IREQ, Hydro Québec, Manicouagan, Canada, Nov. 1995, pp. 95-279. (in French)
9. Javanmardi, F.; and Léger, P., "Grouting of cracks in concrete dams: numerical modelling and structural behaviour," Progress in Structural Engineering and Materials, 2005, V. 7, pp. 161-173.
10. Lombardi, G., "The role of cohesion in cement grouting of rock," International

Commission on Large Dams (ICOLD), 15<sup>th</sup> Congress, Q. 58, R. 13, Lausanne, Switzerland, 1985, pp. 235-261.

11. Nguyen, V.-H.; Remond, S.; and Gallias, J.-L., "Influence of cement grouts composition on the rheological behaviour," *Cement and Concrete Research*, V. 41, No. 3, Mar. 2011, pp. 292-300.

12. Raphael, J. M., "Tensile Strength of Concrete," *ACI Journal proceeding*, V. 81, No. 2, Mar. 1984, pp. 158-165.

13. Nianxiang, X.; and Wenyan, L., "Determining Tensile Properties of Mass Concrete by Direct Tensile Test," *ACI Materials Journal*, V. 86, No. 3, 1989, pp. 214-219.

14. Chandra, K. J.; and Subba, R. P., "Fracture of cold jointed concrete interfaces." *Engineering Fracture Mechanics*, 2007, V. 74, pp. 122-131.

15. ASTM C78 "Standard Test Method for Flexural Strength of Concrete (Using Simple Beam with Third-Point Loading)," ASTM International, West Conshohcken, PA, 2002. 3 pp.

16. ASTM C192 "Standard Practice for Making and Curing Concrete Test Specimens in the Laboratory," ASTM International, West Conshohcken, PA, 2002. 8 pp.

17. ASTM C469 "Standard Test Method for Static Modulus of Elasticity and Poisson's Ratio Concrete in Compression," ASTM International, West Conshohcken, PA, 2002. 5 pp.

18. Khaloo, A. R.; Mohamadi Shooreh, M. R.; and Askari, S. M., "Size Influence of Specimens and Maximum Aggregate on Dam Concrete: Compressive Strength," *Journal of Materials in Civil Engineering*, 2009, V.21, No. 8, pp. 349-355.

19. Lombardi, G.; and Deere, D., "Grouting design and control using the GIN principle," *Water Power & Dam Construction*, Jun. 1993, pp. 15-22.

20. Hydro Quebec, "Injection report of the plunging crack in the arch 6-7 of the Daniel-Johnson Dam," Hydro Quebec Report, Dams and Civil Work, Manicouagan Region, Manicouagan, Quebec, Canada, 2008. 90 pp. (in French)

21. ASTM C940 – 98a “Standard Test Method for Expansion and Bleeding of Freshly Mixed Grouts for Preplaced-Aggregate Concrete in the Laboratory,” ASTM International, West Conshohocken, PA, 2003. 2 pp.
22. ASTM D6910 “Standard Test Method for Marsh Funnel Viscosity of Clay Construction Slurries,” ASTM International, West Conshohocken, PA, 2004. 3 pp.
23. ASTM C579 “Standard Test Method for Compressive Strength of Chemical-Resistant Mortars, Grouts, Monolithic Surfacing, and Polymer Concretes,” ASTM International, West Conshohocken, PA, 2001. 4 pp.
24. ASTM C496 “Standard Test Method for Splitting Tensile Strength of Cylindrical Concrete Specimens,” ASTM International, West Conshohocken, PA, 2004. 5 pp.
25. ASTM C39/C 39M – 03 “Standard Test Method for Compressive Strength of Cylindrical Concrete Specimens,” ASTM International, West Conshohocken, PA, 2002. 5 pp.
26. Bazant, Z. P.; and Pfeiffer, P. A., “Shear fracture tests of concrete,” *Matériaux et Construction*, V. 19, No. 110, Feb. 1986, pp. 111-121.
27. Holcim, “The micro-cement designed for oil well cementing, soil and rock consolidation, rehabilitation of damaged structures and high-performance solutions,” Catalogue Holcim, France, 2008. 20 pp.

## CHAPTER 4      COMPLEMENTARY RESULTS AND GENERAL DISCUSSION

Chapter 4 discusses the development of the concrete mix for the specimen construction, the rheological tests done on the grout, the design and reasoning behind the test method used and describes the injection procedure in detail. Complimentary data obtained during the experimental research is also presented. Finally, future research in this area is presented.

### 4.1 Development of Concrete Mix

The mass concrete mix used for the experimental research was based on the BDJ mass concrete mix (Table 4-1). BDJ concrete used low heat of hydration cement to reduce the temperature increase during curing of the dam. In the case of BDJ the slower curing times were deemed acceptable. Ice and cooling pipes circulating cold water were also used in the concrete mix and its placement to reduce the initial temperature of the dam so that maximum cement hydration temperatures would be reduced. This was done to reduce the likelihood of excessive thermal gradients inducing cracking and other effects of thermal stresses including delayed shrinkage in contraction joint grouting to ensure arch action in the dam (Bulota et al., 1991).

Table 4-1: 1967-68 BDJ Concrete Mix

Material	1000 L	
Cement*	234	kg
Large Sand	364	kg
Fine Sand	363	kg
Aggregate 20-10	148	kg
Aggregate 38-20	231	kg
Aggregate 75-38	445	kg
Aggregate 150-75	534	kg
Water**	113	kg
entrained air	0.3	kg

\* LH, \*\*Frozen (Ice)

In the case of this experimental study, general use cement was used. This was done because thermal stresses were not a concern for small specimens and a quick curing time was beneficial to complete the experimental research in a timely manner. Additionally, using general use cement in lieu of low heat cement will have a negligible effect on the mechanical properties and strengths of the specimens for the purpose of this study (Vagn, Peter, & Paul, 2006).

The maximum aggregate size feasible in the laboratory was 100 mm. This is due to the fact that if an aggregate size of 150 mm was used in accordance to the actual BDJ concrete mix, to satisfy the ratio of maximum aggregate size to specimen dimensions size, it would require specimens with a volume of roughly 650 liters (ASTM, 2002c). The concrete mixer used had a volume of roughly 550 liters which would be insufficient to accommodate the larger pouring volumes that would have been required.

The first step in modifying the BDJ concrete mix was to reallocate the weight of aggregates larger than 100 mm to the rest of the weight of the mix. Three separate mixes from the redistributions are seen in Table 4-2: mix 1, mix 2, and mix3. For mix 1, the weight of the aggregates in the 150 mm to 75 mm bracket was assigned to aggregates in the 75 mm to 38 mm bracket. For mix 2, the weight of the aggregates in the 150-75 mm bracket was distributed over the weight for all the grain sizes equally (including sand). For mix 3, the weight of aggregates in the 150 mm to 75 mm brackets was distributed over all the other aggregates (excluding sand). For the first mixes, the largest aggregate bracket available without exceeding 100 mm was 38 mm to 75 mm. Aggregates of 50 mm to 100 mm were obtained for future mixes. The percentage passing vs. grain size (log) for each mix can be seen in Table 4-3 and was plotted Figure 4-1. Mix 3 showed the smoothest curve and was chosen to continue the concrete mix development.

Table 4-2: Mix1, 2, and 3

Aggregate		$\rho$ [kg/m <sup>3</sup> ]		
Diameter mm	Original BDJ 1967-1968	Mix 1	Mix 2	Mix 3
150 - 75	534	0	0	0
75 - 38	445	979	552	623
38 - 20	231	231	338	409
20 - 10	148	148	255	326
Large Sand (5)	364	364	471	364
Fine Sand (2)	363	363	470	363
Total	2085	2085	2085	2085

Mix 1: 150 - 75 mm aggregate weight moved to 75 - 38 mm aggregate

Mix 2: 150 - 75 mm aggregate weight moved distributed over aggregates and sand

Mix 3: 150 - 75 mm aggregate weight moved distributed over aggregates only

Table 4-3: Sieve Analysis

Sieve	Original	Percent Passing		
		Mix 1	Mix 2	Mix 3
150.0 mm	100	100	100	100
75.0 mm	74.39	100	100	100
38.0 mm	53.05	53.05	73.53	70.12
20.0 mm	41.97	41.97	57.33	50.50
10.0 mm	34.87	34.87	45.11	34.87
5.0 mm	17.41	17.41	22.53	17.41
2.0 mm	0.00	0.00	0.00	0.00

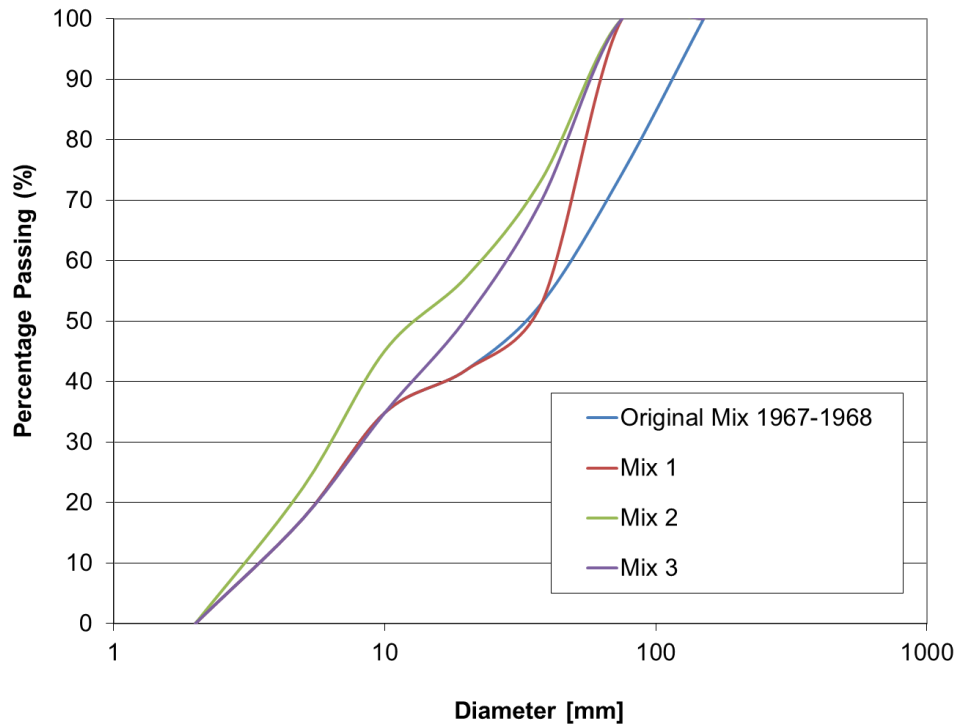


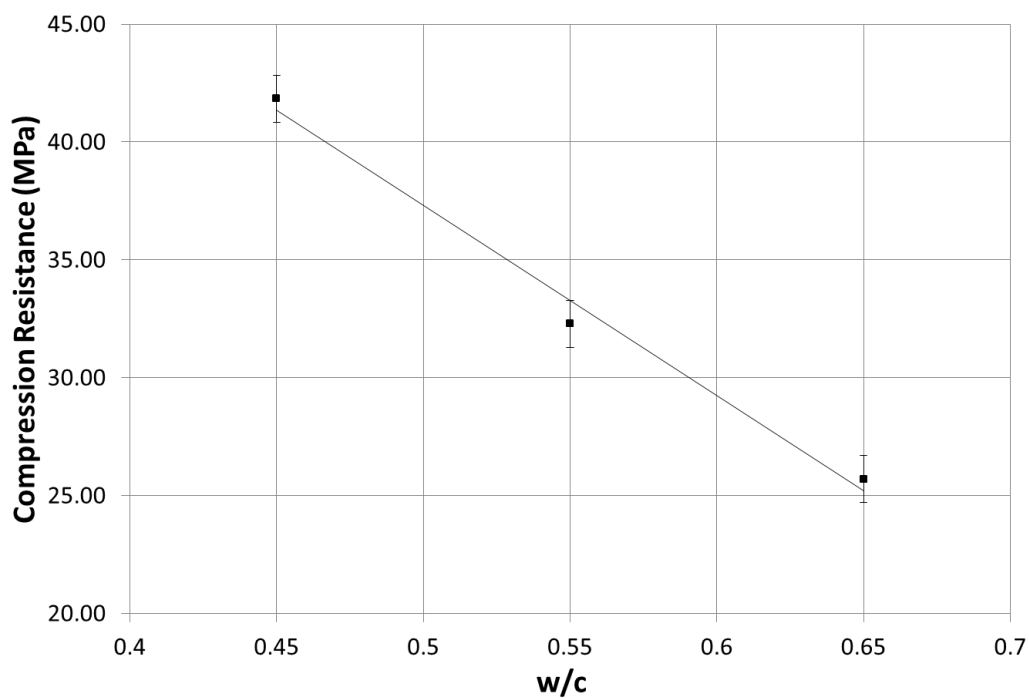
Figure 4-1: Granulometric Curve

The next step was to determine the w/c ratio needed to achieve a compressive strength of 30 MPa, the initial design compressive strength of BDJ concrete. Three concrete mixes derived from Mix 3 were developed. They have the same paste/aggregate ratio as Mix 3 but have separate w/c ratios. The w/c ratios chosen were 0.45, 0.55, and 0.65. Six inch cylinders of the half scale mixes seen in Table 4-4 were then tested in compression following ASTM C39 (2002). The results of these tests were graphed as compressive strength vs. w/c ratio. From Figure 4-2, a w/c ratio of approximately 0.6 corresponded to a compressive strength of 30 MPa.



Table 4-4: Small Scale Concrete Mixes

	w/c					
	0.45		0.55		0.65	
	Mass kg	Volume L	Mass kg	Volume L	Mass kg	Volume L
Cement	16.75	5.32	14.82	4.70	13.29	4.22
Sand	49.90	18.48	49.90	18.48	49.90	18.48
2.5 - 10 mm	22.38	8.29	22.38	8.29	22.38	8.29
10 - 20 mm	28.07	10.40	28.07	10.40	28.07	10.40
20 - 40 mm	42.76	15.84	42.76	15.84	42.76	15.84
Water	7.54	7.54	8.15	8.15	8.64	8.64
Admixture	0.02	0.02	0.02	0.02	0.02	0.02
(Air)	0.00	4.12	0.00	4.12	0.00	4.12
Total	167.42	70.00	166.11	70.00	165.06	70.00

Figure 4-2: 28 Day  $f_c'$  (small scale mix)

Scaling back up to normal size, Mix A, seen in Table 4-5, was chosen. The aggregate sizes were modified slightly based on available aggregates. Three 400 x 800 mm cylindrical specimens were poured at the University of Sherbrooke. The mix was very difficult to pour and had little workability. Vibration had very little effect on the concrete. The Specimens were transported to Ecole Polytechnique of Montreal to be tested in compression in a 12 MN MTS Actuator. Because the concrete was not workable, and vibration had little effect, upon opening the tubes many large air pockets were observed. One of the samples was not tested because of the quantity of air pockets. After testing only two of the samples, the mix had an average compression resistance under 25MPa.

Table 4-5: Mix A

Material	1000 L	
Cement	200.17	kg
Sand	712.88	kg
10 - 20 mm	319.67	kg
20 - 40 mm	401.06	kg
50 - 100 mm	610.9	kg
Water	120.1	kg
Admixture AEA	0.45	kg
(Air)	0	kg
Superplasticizer	0.9	kg

The concrete mix needed to be vastly improved so that it could be properly poured. To this end, a compressive packing model with parameters defined by Willem (2006) was used to optimise the granulometry. A w/c ratio of 0.6 and an initial density of cement were used as the starting parameters. Additionally, the specific granulometric breakdown of each aggregate bracket was needed. The model then uses this information to determine the optimal required weight of each aggregate bracket. It did so by modeling and optimizing the stacking of the aggregates. Two mix options were developed: Option I, with 300 kg/m<sup>3</sup> of cement and Option II, with 250 kg/m<sup>3</sup>. Option I was a conservative mix with more cement and water to try to ensure a more workable end product. Option II used less cement and less water to try and obtain a stronger concrete. Three 400 x 800 mm cylindrical specimens were poured for each mix, again at the Université de Sherbrooke. The two mixes can be seen in Table 4-6. The Compressive strength for the two

mixes was 22 MPa and 25 MPa respectively. Both Options were workable, as expected Option II was more workable, however the compressive strength of both mixes was too low.

Table 4-6: Stacking Model Mixes

Material	1000 L		
	Option I	Option II	
Cement	300	250	kg
Sand	650	675	kg
5 - 10 mm	260	305	kg
10 - 20 mm	220	220	kg
20 - 40 mm	340	345	kg
50 - 100 mm	400	450	kg
Water	180	150	kg
Admixture AEA	0.45	0.45	kg
(Air)	0	0	kg
Superplasticizer	0.9	0.9	kg

The final mass concrete mix, seen in Table 4-8, was chosen. To obtain this mix, the aggregate, sand, and water content from Option II stayed identical however, to increase the strength of the concrete it was decided to decrease the w/c ratio from 0.6 to 0.53 by simply increasing the quantity of cement used. Three batches of the concrete were poured due to the limitations of the volume of the mixer. The slump and spread of the first batch was too high and there was a worry of excessive bleeding. Because of this, the quantity of superplasticizers was decreased for batches 2 and 3 to try and improve the concrete. Table 4-7 has a summary of the results of the rheological tests done on all three batches of concrete. The slump and spread for batch 3 were significantly lower than for batches 1 and 2. This was due to an error in mixing order for batch 3 in which the superplasticizers was added prior to water. Because of this, the superplasticizer was absorbed by the dry aggregates and thus was not able to be properly mixed, decreasing its efficiency. The slump, spread, density, and air tests were done on concrete sieved to 20 mm. This decreased the density from the expected value of 2408 kg/m<sup>3</sup>.

Table 4-7: Wet Concrete Properties

Batch	Slump mm	Spread mm	Temperature °C	Air %	Density kg/m <sup>3</sup>
1	250	550-540	25	4.2	2339.5
2	190	370-360	26.2	4.7	2288.4
3	60	210-200	26	6.8	2232.1
Average	167	377-367	25.7	5.2	2286.1

Table 4-8: Final Experimental Mix

Material	1000 L	
Cement	270	kg
Sand	675	kg
Aggregate 5-10	305	kg
Aggregate 10-20	220	kg
Aggregate 20-40	345	kg
Aggregate 50-100	450	kg
Water	143	kg
AEA	770	ml
Eucon® 37	3090/2730*	ml

\* Batch 2 and 3

## 4.2 Grout Rheology

The following tests were done on the liquid grout and the results can be found in Chapter 3:

- Density – C905-01(2012) Standard Test Methods for Apparent Density of Chemical-Resistant Mortars, Grouts, Monolithic Surfacing, and Polymer Concretes;
- Bleeding – ASTM C940-98a Standard Test Method for Expansion and Bleeding of Freshly Mixed Grouts for Preplaced-Aggregate Concrete in the Laboratory [Figure 4-3 (a)];
- Flow Time – ASTM D6910-04 Standard Test Method for Marsh Funnel Viscosity of Clay Construction Slurries [Figure 4-3 (b)];
- Set Time – Thermocouple [Figure 4-3 (c)].



(a)



(b)



(c)

Figure 4-3: Grout-Rheological tests: (a) Bleeding, (b) Cone Marsh, (c) Thermocouple

The set time test involved mounting a thermocouple, which measures the temperature every 10 minutes, at the center of a 75 x 150 mm cylinder. Once the grout was properly mixed, it was then poured into this cylinder. The ambient temperature was also measured every 10 minutes. The temperature of the grout was then plotted against the time from initial mixing of the grout. The set time was then measured as the time it took for the maximum temperature to be obtained, which is the point at which much of the hydration reaction has taken place and when the grout has reached initial set (Saleh et al., 1997). Figure 4-4 is a typical graph for the results of the set time.

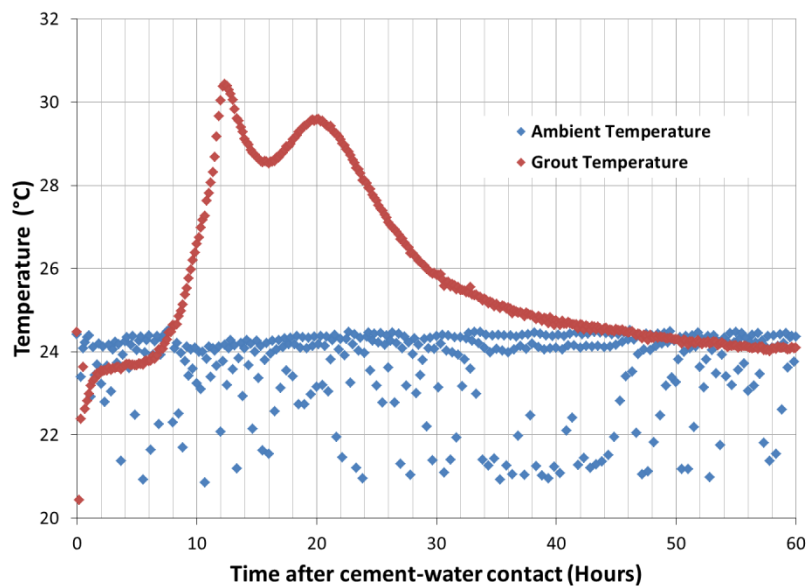


Figure 4-4: Typical Thermocouple Results

### 4.3 Test Method Design

Concrete's tensile resistance is not as straightforward as its compressive resistance. The tensile resistance for concrete is not a constant material property; it changes depending on the way that the specimen is loaded. There are many available tests to determine the tensile resistance of unreinforced concrete. These tests include direct tensile test, splitting test (Brazilian), third point loading test (modulus of rupture), and the wedge splitting test. The relationship between compressive resistance and the tensile resistance found for the different tests are discussed in Chapter 3.

### 4.3.1 Direct Tension

A direct tensile test consists of pulling a concrete specimen in direct tension till failure occurs. This can be done in many different ways, a few of which are discussed here.

One method is to pour the specimen with rods embedded both end. Both ends of the specimen can then be attached to an actuator and pulled apart in direct tension. Although this method seems like it would yield the best results, there are many obstacles when using this method. It is important to make sure the rods do not pull out and that there is a sufficient distance between the rods and the center of the specimen so that the tensile force can properly develop. This method is also difficult to use because it is very difficult to have a perfect alignment of the bars, this will cause an eccentricity of the forces and may influence the resistance of the specimen. Even if the bars are perfectly aligned, there may also be an eccentricity in the actuator which would lead to the same problem. Additionally, in the case of mass concrete specimens, due to the large aggregate size, there is little space available for the bars (Raphael, 1984; Wang & Song, 2009).

It is also possible to use clamps on the 4 sides of the two ends of the specimens and to pull from these clamps. The problem with this method is that a significant compressive force is created in the two ends of the specimens. This change in stress-strain state may have an effect on the tensile resistance of the concrete (Wang & Song, 2009).

It is also possible to use an epoxy glue to attach each end of the specimen to a metal plate which can then be attached to an actuator. To use an epoxy binder, the two end faces need to be perfectly aligned and well finished and the metal plates need to be perfectly centered.

Again with all of these methods, there is a risk of eccentricities which typically leads to inaccurate results (Raphael, 1984).

### 4.3.2 Splitting Test

The Brazilian test is done on cylindrical specimens. The general approach is to lay the cylinder on its side and apply a compressive force along its entire length. This in turn will create an indirect tensile force along the central plane which will split the cylinder in two. To do this test, ASTM C496 (2011) requires specimens larger than 150 mm diameter because at the point of application of the load, the compression force restrains the specimen and causes a local change in

the stress-strain distribution which can lead to erroneous results. In the case of mass concrete, this size requirement does not pose a problem however; there are difficulties that would arise with a large specimen. Placing a large cylindrical specimen on its side with precision, and ensuring a level and true contact between the specimen and the mechanism applying a force would prove problematic. As well, to repair this type of specimen with the micro fine cement grout used, without disturbing the crack area would not be ideal.

### **4.3.3 Modulus of Rupture**

ASTM C78 (2002), Standard test method for flexural strength of concrete (using a simple beam with using third point loading) was deemed the most appropriate tensile test for this experimental research. The test involves placing the beam on a support at either end and applying two equal loads at third points. The advantage of C78 is the fact that the moment will be equal along the center third of the beam. The moment that is applied to the beam creates a compressive force in the top of the beam and tension in the bottom with an assumed linear stress distribution between the two. The beam will fail when the tensile force in the most bottom section of the beam exceeds the tensile resistance of the concrete. The modulus of rupture at failure can then simply be calculated by applying classical strength of material behaviour laws (ASTM, 2002b).

Here are some of the advantages which lead to this test method being chosen. The specimen required for this test is a simple beam specimen. The test is easily reproducible and is highly documented. This test also gives accurate results and results which are closest to the results obtained from numerical modeling (Raphael, 1984). Additionally, both ends of the specimen are supported which allowed easy access to the center of the specimen for the purpose of repairing it.

## **4.4 Injection Procedure**

Prior to testing a specimen that was to be repaired, an exit hole was drilled. This hole passed at an angle from the center of the specimen to the top surface of the specimen around one quarter of the distance to the end. A valve (A) was then attached to this exit hole. A pipe piece fitted with a pressure meter was attached to the valve (A). A final valve (B) was attached to this pipe piece as seen in Figure 4-5 (a).

Prior to the injection process, the crack width needed to be set to a fixed value, in this case 2 mm was chosen. This was done as described in Chapter 3.

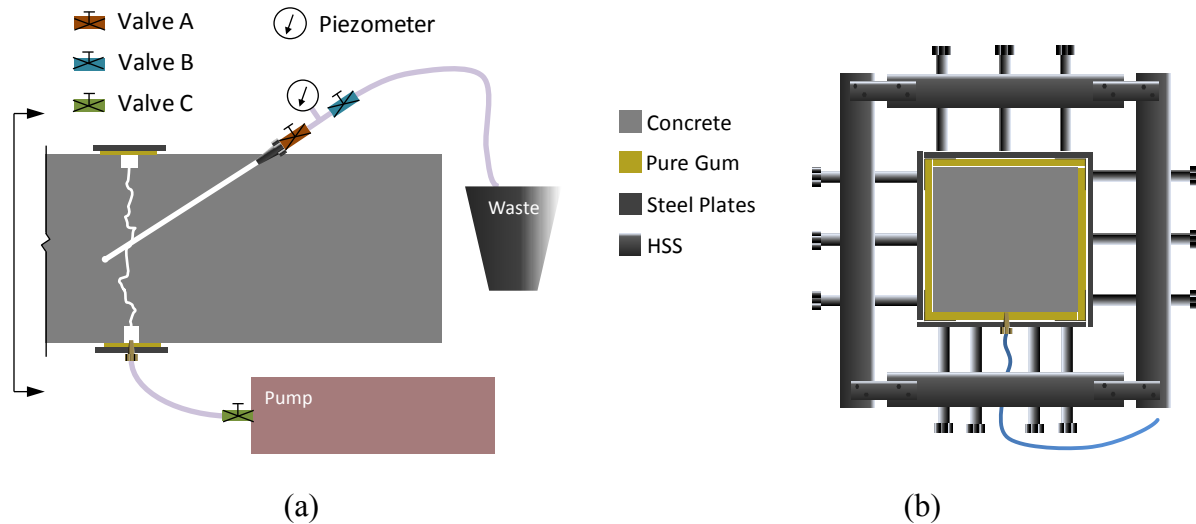


Figure 4-5: Injection: (a) Injection Flow Path, (b) Injection Frame

The injection needed to be maintained under a constant pressure of roughly 0.2 MPa. To do this, the frame seen in Figure 4-5 (b) was used. A layer of pure gum was placed against the specimen. When under pressure, the pure gum had a tendency to deform through the corners and let the injection liquid escape. To prevent this, four thin steel plates bent at 90 degrees were placed over top of the pure gum in the corners. Four steel plates were then placed over top of the pure gum. A steel frame consisting of four HSS was then mounted around the specimen. Holes were pre-drilled through the HSS and fitted with bolts to allow one-inch rods to be screwed through the frame. The four steel plates were held tightly against the pure gum by tightening the rods.

Pure gum was chosen because it has very little relaxation as opposed to a standard rubber. If a standard rubber was used, once the injection material under pressure, the rubber would relax and over time, the injection fluid could leak out.

Once the frame installed, a tube attached to the injection pump was fitted to a pre-drilled hole in the bottom of the injection frame. A manual injection pump was used to first pass water through the crack. Once the water exited the specimen from the exit hole, the valve (B) was shut off and the pressure was increased to 0.2 MPa. The pressure meter was checked every 15 minutes. If the pressure decreased below 0.2 MPa, the pump would be used to increase the pressure. This was done till a constant 0.2 MPa was reached with no additional pumping. The pressure decrease is normal due to the two pieces of concrete moving apart and due to the water being absorbed by the concrete. The water was left in the specimen for 24 hours. At this point water was once again



flushed through the system. Finally, grout was pumped through the specimen. Once the quality of the grout, by visual inspection, exiting the specimen was the equivalent to the grout being pumped into the specimen, the exit valve (B) was shut until a pressure of 0.2MPa was reached. The pressure was increased every 15 minutes as needed. After one hour, the pressure remained constant. Valve (A) was shut 1 hour later so that the pressure meter could be removed and cleaned.

## 4.5 Complementary Load-Displacement Data

### 4.5.1 Modulus of Rupture

Much additional data was collected during the experimental testing. Two LVDTs were used to measure the deflection of the specimens and four LPs with a gauge length of 150 mm were also fixed to the specimens during testing. One was placed at the center of the top, bottom, north, and south face of the specimen respectively. They were used to measure the progression of the opening of the crack on all four sides of the specimen as seen in Figure 4-6.

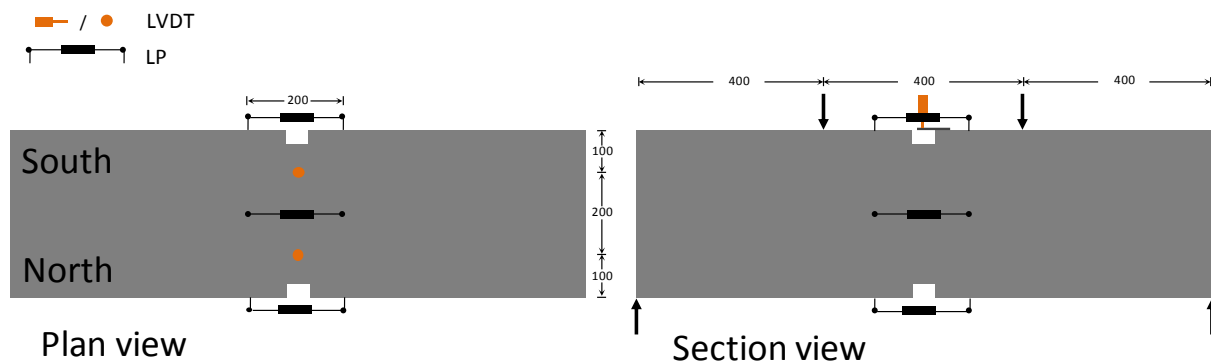


Figure 4-6: Modulus of Rupture Instrumentation

The progression of the crack opening was used during the tests to be able to note any particularities such as excessive eccentricities. It was also measured for future research, to help with the validation and verification of numerical models. Figure 4-7 (a) and (b) are examples of typical curves for load vs. north-south crack opening and load vs. top-bottom crack opening respectively. The absolute value of the crack opening for the top of the specimen was taken as the value recorded was negative because the crack was getting smaller. The absolute values obtained from the LPs can be found in Table 4-9.

As can be seen from Figure 4-7 (a), the slope of the bottom and top curves follow each other very well until the 50 kN mark is reached. At this point the bottom crack opens much more than the top crack compresses. This is to be expected since the top portion of the specimen is still within the elastic range because concrete has a much large compressive force than tensile force. This graph can also help explain why the modulus of rupture test tends to overestimate tensile strength (Raphael, 1984).

As seen from Figure 4-7 (b), as expected, since this opening is measured along the assumed neutral axis of the specimen the displacement that occurs at the center of the two vertical faces is roughly zero. Again, in reality, the neutral axis has a tendency to move towards the top of the specimen which explains why the central portion of the specimen does deform horizontally. The difference from one side of the specimen to the other is virtually equal to zero with the largest difference found to be roughly five one thousandths of a millimetre. A difference is expected as concrete is a heterogeneous material and the simple positioning of the aggregates within the specimen can account for some discrepancies between the crack openings on either side.

Table 4-9: Modulus of Rupture Results

Specimen #	Test #	W/C	Max. Force [kN]	$\Delta$ – Max. South [mm]	$\Delta$ – Max. North [mm]	$\Delta$ – Max. Avg. [mm]	Max. Stress [MPa]
A	1	N/A	119.8	0.483	0.487	0.485	3.35
A	2	1	17.4	0.162	0.057	0.109	0.49
A	3	1	21.6	0.135	0.056	0.095	0.61
B	1	N/A	98.2	0.451	0.432	0.435	2.75
B	2	0.5	33.4	0.129	0.120	0.124	0.93
B	3	0.5	33.1	0.106	0.096	0.101	0.93
C	1	N/A	88.8	0.352	0.355	0.353	2.49
D	1	N/A	110.2	0.365	0.356	0.361	3.08
E	1	N/A	92.3	0.304	0.223	0.264	2.58
F	1	N/A	88.9	0.321	0.300	0.310	2.49
Avg. for	1		100	0.379	0.359	0.368	2.79
Avg. for	2		25	0.145	0.088	0.117	0.71
Avg. for	3		27	0.120	0.076	0.098	0.77
Avg. for		0.5	33	0.117	0.108	0.113	0.93
Avg. for		1	20	0.148	0.056	0.102	0.55

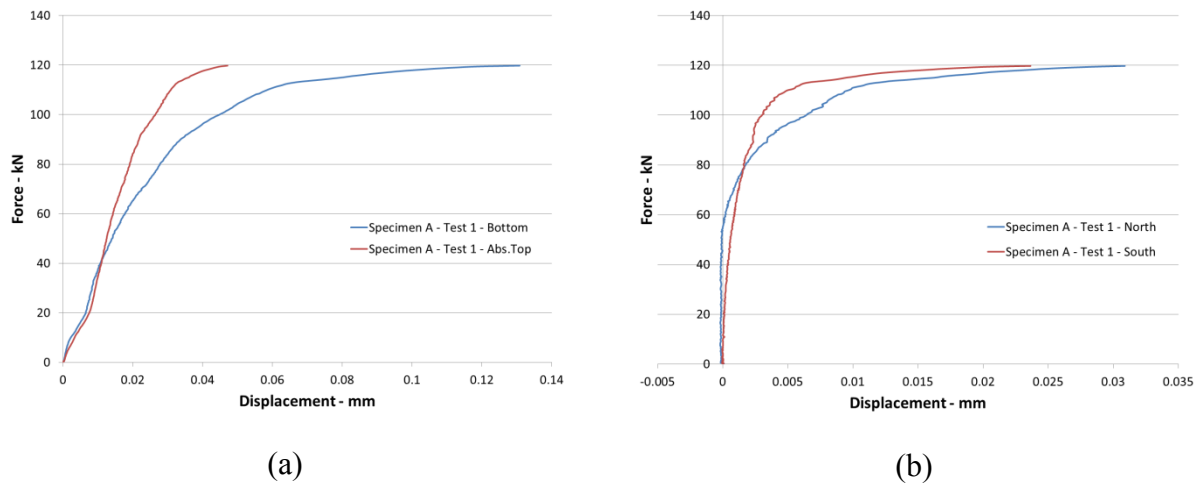


Figure 4-7: Crack Opening: (a) Bottom/Top, (b) North/South

#### 4.5.2 Shear Test

In the case of the shear test, six LVDTs were used to measure the deflection, three on either side of the specimen. Two were placed over the hanging edge, two were positioned over the reaction, and two were positioned over the applied load. Again, four LP's were used to measure crack opening however, for this test two were placed on each vertical face. The positioning of the different measurement devices can be seen in Figure 4-8. Typical load vs. measured deformation graphs for two tests can be seen in Figure 4-9.

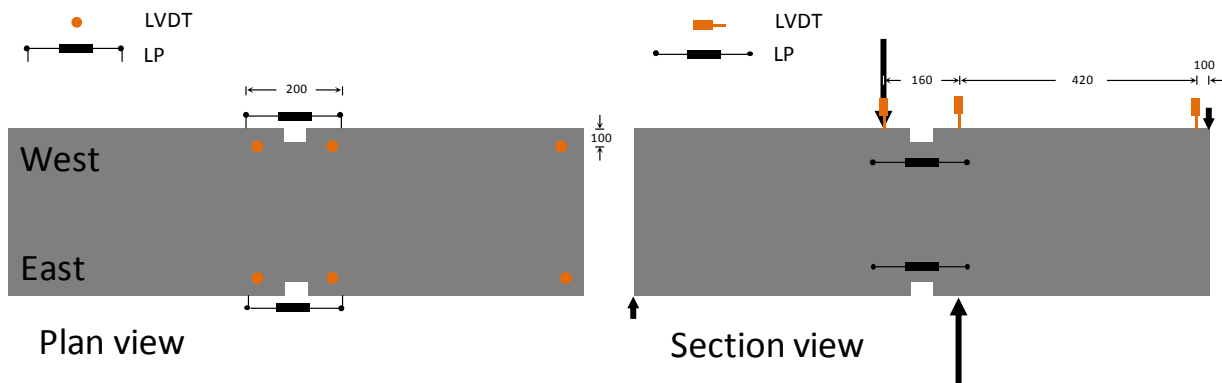
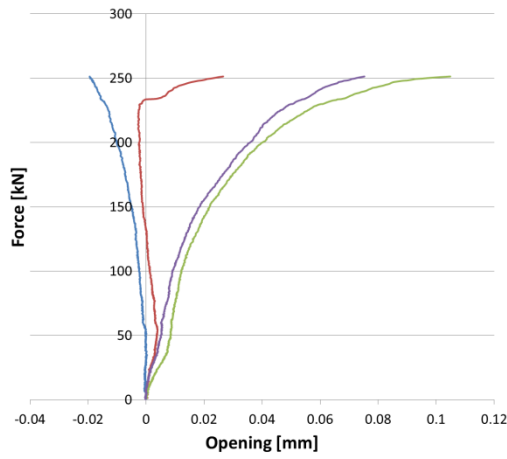
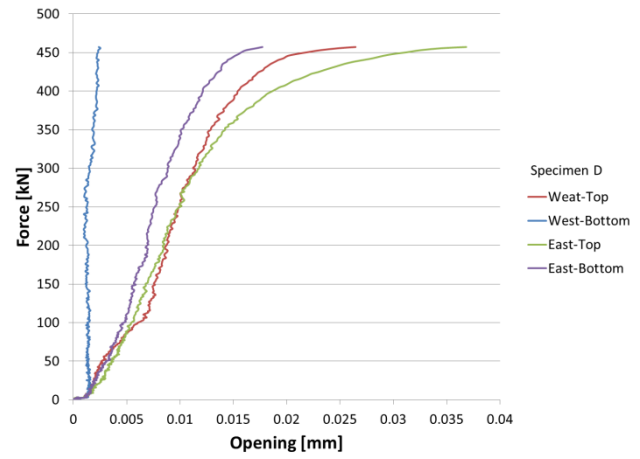


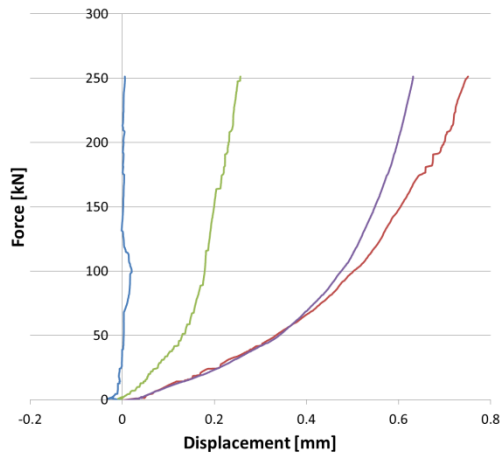
Figure 4-8: Shear Test Instrumentation



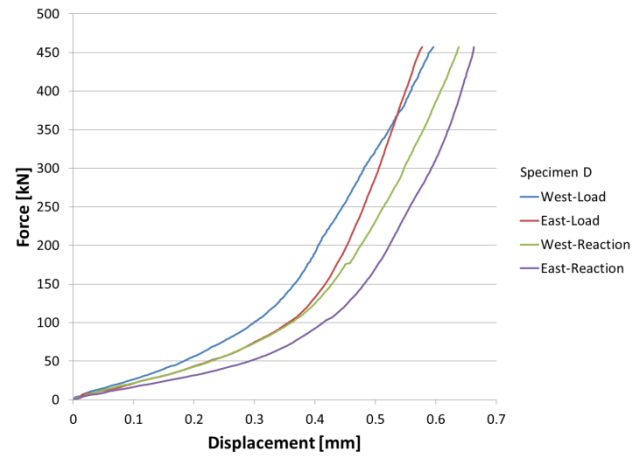
(a)



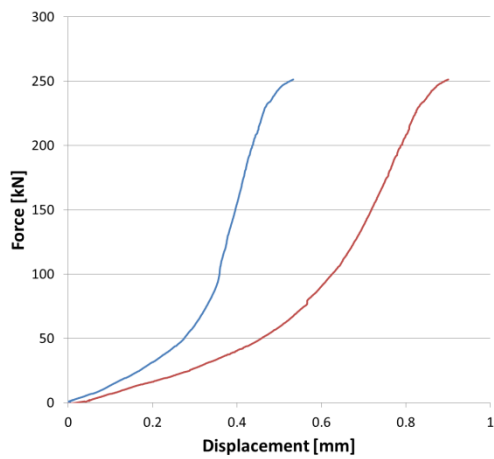
(d)



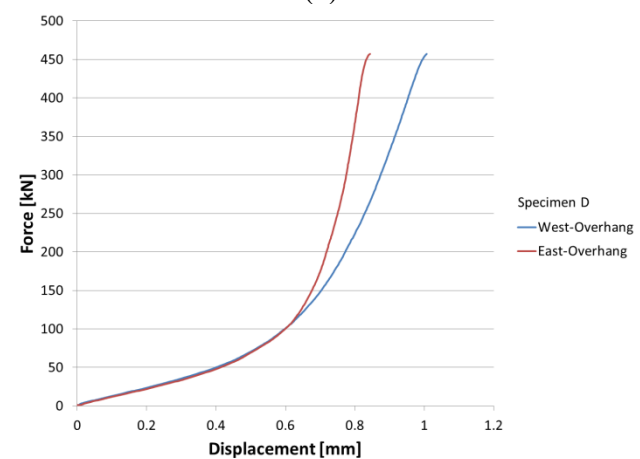
(b)



(e)



(c)



(f)

Figure 4-9: Load vs. Deformation: (a) Crack Opening B, (b) Center Deflection B, (c) Overhang B, (d) Crack Opening D, (e) Center Deflection D, (f) Overhang D

This data was again measured to be able to track the evolution of the specimen deformations and crack openings during the tests. It can also be beneficial for future work involving numerical modeling. The relatively large difference in displacement on opposing sides of shear specimens noted in Figure 4-9 suggests much more eccentricity in the shear test than in the modulus of rupture test. This can be explained because firstly, the actuator used to apply the load was not hinged in the east west direction. The second factor explaining these eccentricities is that the measurement devices are relatively close to the main loading point and reaction which means that stress concentrations may play a role in the displacements measured. Since these tests were done for comparative purposes and there was an insufficient quantity of specimens to obtain statistically accurate results, it was deemed that this error was acceptable.

## 4.6 Prospective Future Work

### 4.6.1 Experimental

This research work forms a foundation for similar tests to be conducted in the future. Now that a working experimental protocol exists to test repaired mass concrete specimens, more in depth research in this area can be done.

To develop the Mohr-Coulomb shear failure envelope, the shear test can be reproduced with the addition of a normal force. An actuator as seen in Figure 4-10 can be used to maintain different constant normal forces.

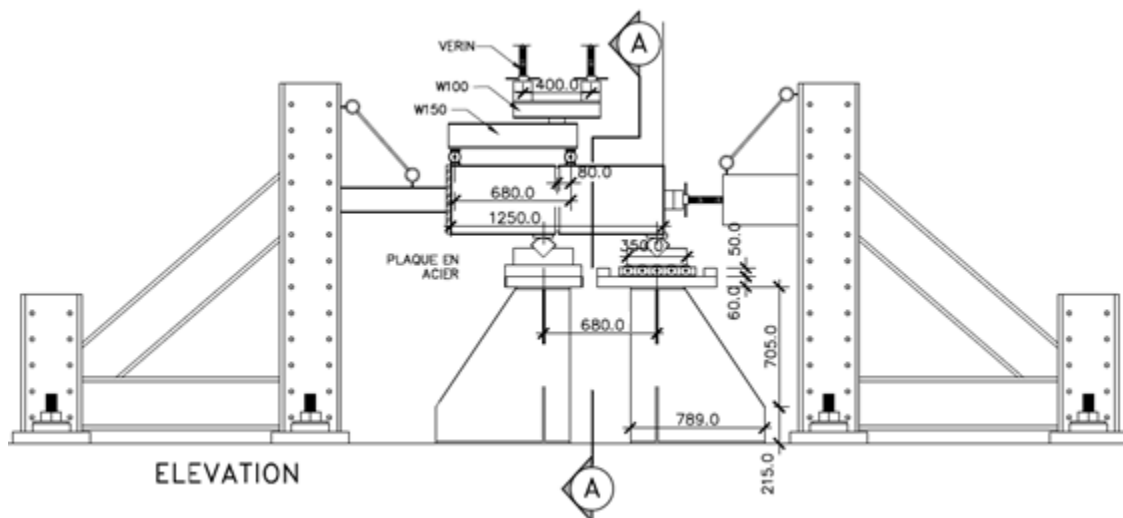


Figure 4-10: Potential Future Shear Test with Normal Force



the results found can be used for the refinement of actual dam numerical models in which the tensile resistance of repairs is currently assumed null. These results can also be used to help to assess the sensitivity of numerical model results dealing with different loading scenarios and injection scenarios for mass concrete dams.

## CONCLUSIONS

The largest multiple-arch dam in the world, Daniel-Johnson dam, located in northern Quebec has experienced multiple types of cracks since the end of its construction in 1968. Extensive research has been done to determine the penetrability and injectability of different injection grouts. The rheology and behaviour of different injection materials has been the focus of many studies; however, the mechanical resistance provided to the injected area is an aspect of the injection process that has been neglected. Because of this lack of knowledge, it is assumed that the repairs done to repair BDJ provide no tensile or shear resistance. This assumption leads to a loss of potential reservoir capacity.

The main objective of this experimental research was to determine the tensile and shear resistance of dam mass concrete repaired one time or multiple times by grout in injection with grouts with w/c ratios of 0.5 and of 1.0. The objectives were to determine a mass concrete mix, develop an experimental protocol to test the un-cracked and repaired mass concrete, to develop an injection process, and determine their tensile and shear resistance.

For the experimental investigation, the following conclusions can be drawn:

The mass concrete mix developed, with maximum aggregate size of 100 mm, has a compressive strength of 28 MPa, which is representative of BDJ mass concrete mix. The modulus of rupture of the mass concrete mix used was equal to 2.8 MPa which was roughly 10% of its compressive strength.

The modulus of rupture of a repair specimen is related to the w/c ratio of the injection grout, or the injection grouts adhesion. With a lower w/c ratio, a better adhesion occurs between the injection grout and the concrete. It was found that a w/c ratio of 1.0 and 0.5 lead to a modulus of rupture of 0.5 and 1.0 MPa or 15% and 30% of the original modulus of rupture respectively.

It was also found that multiple repairs with the same grout type had no effect on the strength of the repair. In other words, a specimen repaired once or two times with the same type of grout had the same modulus of rupture.

The failure plane for the modulus of rupture test occurred at the interface of the concrete and the repair grout. The path of this failure plane was dependent on the aggregate placement. The failure



plane tended to circumvent large aggregates and seemed to jump from one concrete-grout interface to the other concrete-grout interface when intersected with a large aggregate.

The shear resistance of the repaired mass concrete specimen was found to vary between 0.57 MPa and 3.73 MPa and was a function of two factors: the repair grouts w/c ratio as well as the width of repair grout layer. These two factors also played a role in the failure planes observed during testing.

As with the modulus of rupture test, a lower w/c ratio leads to a higher shear resistance again because of a higher adhesion between base material and repair material.

Multiple repairs, in the case of shear strength, do have an effect on strength. Multiple repairs lead to thicker grout layers, this increased thickness decreases the shear resistance found.

Two main failure types were observed: (i) a single crack at the grout-concrete interface and (ii) a crack at the grout-concrete interface with a crack going through un-cracked concrete going from the loading point to the reaction point.

For the failure plane occurring at the grout-concrete interface, the same failure pattern as for the modulus of rupture was observed, with the large aggregates influencing the path of the failure plane. For the crack occurring in the previously un-cracked concrete, the failure plane tended to shear through all aggregate regardless of size.

When a specimen was repaired only once and with a grout having w/c ratio of 0.5, failure mode (ii) was observed with a resistance of 3.73 MPa. This can be attributed to the fact that the concrete grout interface is stronger with a w/c ratio of 0.5 and having a thin layer of grout leading to the development of crack between the load and reaction.

When a specimen was repaired three times and with a grout having a w/c ratio of 1.0, failure mode (i) was observed with a resistance of 0.57 MPa. This can be attributed to the fact that the concrete grout interface is weakest with a w/c ratio of 1.0 and having a thick layer of grout leading to the failure first occurring at this interface.

When a specimen was repaired once and with a grout having a w/c ratio of 1.0 or three times and with a grout having a w/c ratio of 0.5, a hybrid failure mode in between (i) and (ii) was observed with a resistance of roughly 2.4 MPa.

These results are important for structural applications. A resistance of 1 MPa to 0.5 MPa in traction is significant for mass concrete dams and would represent roughly 100 m to 50 m of water head (however, the relationship between the stress field near a crack tip and the water head is not linear). Additionally, 3.5 MPa to 0.5 MPa shear resistance is significant for mass concrete dams. Both the shear and tensile strength provided by grout injection repairs could be depended on for the prevention of crack propagation.

This research was done on ideal specimens in ideal laboratory conditions; the concrete was not old and the cracks were fresh and clean. In the reality of dam crack repair, it is unlikely to encounter cracks meeting these criteria. Additionally the exact width of the crack, condition of the concrete, and geometry of the crack may not be entirely known. Typically a crack could be exposed to erosion, calcite deposits could form, sedimentation in the crack can occur, or the effects of previously done repairs could be in play. Because of these factors, caution needs to be used when extrapolating the results of this study to practical applications.

## BIBLIOGRAPHY

- Abdel-Maksoud, M. G., Barenberg, E., & Marino, G. G. (2008). *A Proposed New Method for Roughness Quantification of Concrete Joints and Cracks*. Paper presented at the Pavements and Materials Modeling, Testing, and Performance (GSP 184).
- ACI-Committee-207. (1970). *Mass Concrete for Dams and Other Massive Structures*. Paper presented at the ACI Journal Proceedings.
- ACI-Committee-224. (1984). Causes, Evaluation, and Repair of Cracks in Concrete Structures (pp. 453-474). ACI Concrete Repair Manual: ACI.
- Aggelis, D., Shiotani, T., & Polyzos, D. (2009). Characterization of surface crack depth and repair evaluation using Rayleigh waves. *Cement and Concrete Composites*, 31(1), 77-83.
- Allas, É., & Savinskaya, M. (1972). Methods of evaluating the conditions and effect of stabilizing grouting. *Power Technology and Engineering (formerly Hydrotechnical Construction)*, 6(11), 1054-1058.
- Argal, E. (1991). Construction joint grouting characteristics in the dam of the Zeya hydroelectric plant. *Power Technology and Engineering (formerly Hydrotechnical Construction)*, 25(8), 492-499.
- Argal, É., Ashikhmen, V., & Korolev, V. (1972). Experimental work concerning the grouting of joints in the Krasnoyarsk hydroelectric plant dam. *Power Technology and Engineering (formerly Hydrotechnical Construction)*, 6(12), 1155-1161.
- Argal, É., Korolev, V., Kudrin, K., & Ashikhmen, V. (2009). A new material for grouting of joints with small openings in concrete dams. *Power Technology and Engineering (formerly Hydrotechnical Construction)*, 43(6), 337-344.
- Argal, É., & Ryzhankova, L. (1996). Assignment of the initial technological parameters of grouting construction joints of concrete dams. *Power Technology and Engineering (formerly Hydrotechnical Construction)*, 30(8), 450-455.
- ASTM. (2001). C579 - Standard Test Method for Compressive Strength of Chemical-Resistant Mortars, Grouts, Monolithic Surfacing, and Polymer Concretes (pp. 5). West Conshohcken, PA: ASTM International.
- ASTM. (2002a). C39 - Standard Test Method for Compressive Strength of Cylindrical Concrete Specimens (pp. 5). West Conshohcken, PA: ASTM International.
- ASTM. (2002b). C78 - Standard Test Method for Flexural Strength of Concrete (Using Simple Beam with Third-Point Loading) (pp. 3). West Conshohcken, PA: ASTM International.
- ASTM. (2002c). C192 - Standard Practice for Making and Curing Concrete Test Specimens in the Laboratory (pp. 8). West Conshohcken, Pa: ASTM International.
- ASTM. (2002d). C469 - Standard Test Method for Static Modulus of Elasticity and Poisson's Ratio Concrete in Compression (pp. 5). West Conshohcken, PA: ASTM International.
- ASTM. (2003). C940 - 98a - Standard Test Method for Expansion and Bleeding of Freshly Mixed Grouts for Preplaced-Aggregate Concrete in the Laboratory (pp. 2). West Conshohcken, Pa: ASTM International.

- ASTM. (2004a). C496 - Standard Test Method for Splitting Tensile Strength of Cylindrical Concrete Specimens (pp. 5). West Conshohocken, PA: ASTM International.
- ASTM. (2004b). D6910 - Standard Test Method for Marsh Funnel Viscosity of Clay Construction Slurries (pp. 3). West Conshohocken, Pa: ASTM International.
- Axelsson, M., Gustafson, G., & Fransson, Å. (2009). Stop mechanism for cementitious grouts at different water-to-cement ratios. *Tunnelling and Underground Space Technology*, 24(4), 390-397.
- Bažant, Z. (1999). Size effect on structural strength: a review. *Archive of applied mechanics*, 69(9), 703-725.
- Bažant, Z., & Pfeiffer, P. (1986). Shear fracture tests of concrete. *Materials and Structures*, 19(2), 111-121.
- Biggar, K., & Sego, D. (1990). *The curing and strength characteristics of cold setting cement fondu grout*. Paper presented at the Proceedings of 5th Canadian Permafrost Conference.
- Billinghurst, G. (1997). Sealing the draft. *International water power & dam construction*, 49(2).
- Bouja, A. (1995). *Contribution à l'Étude de l'Injection d'un Coulis de Ciment en Milieu Fissuré*. Ph.D., Université de Sherbrooke, Canada, Quebec, Sherbrooke.
- Bremen, R. (1997). The use of additives in cement grouts. *The International Journal on Hydropower & Dams, Volume Four, Issue One*, 71-76.
- Bruce Barrett, P. E., & Ringel, J. (2010). *Upper Stillwater Dam Crack Repair*. Paper presented at the 25th USSD Annual Meeting and Conference Proceedings.
- Bruce, D., & De Porcellinis, P. (1989). *The RODUR Process of Concrete Dam Repair: A Recent Case History*. Paper presented at the Proceedings of the Fourth International Conference on Structural Faults and Repair, London, England.
- Bryzgalov, V., Epifanov, A., Bulatov, V., Permyakova, L., Reinik, O., Stafievskii, V., . . . Rolle, M. (1998). Experience in grouting seeping cracks in the upstream face of the Sayano-Shushenskoe hydrostation dam. *Power Technology and Engineering (formerly Hydrotechnical Construction)*, 32(2), 49-56.
- Bulota, G., Im, O., & Larivière, R. (1991). *Le Barrage Daniel-Johnson: Un Vieillessement Prématuré*. Paper presented at the Proceedings, Seventeenth Congress on High Dams.
- Chandra Kishen, J., & Rao, P. S. (2007). Fracture of cold jointed concrete interfaces. *Engineering fracture mechanics*, 74(1), 122-131.
- Chen, Y., Ye, W., & Zhang, K. (2009). Strength of copolymer grouting material based on orthogonal experiment. *Journal of Central South University of Technology*, 16(1), 143-148.
- Chertykov, Y. D., & Dzhuraev, M. (1983). Experience in grouting concrete under conditions of the far north. *Power Technology and Engineering (formerly Hydrotechnical Construction)*, 17(2), 108-111.
- Chupanit, P., & Roesler, J. R. (2008). Fracture energy approach to characterize concrete crack surface roughness and shear stiffness. *Journal of Materials in Civil Engineering*, 20(4), 275-282.

- Deere, D. U., & Lombardi, G. (1985). *Grout Slurries—Thick or Thin?* Paper presented at the Issues in Dam Grouting.
- Domone, P. (1993). *Structural grouts*: Routledge.
- Draganović, A., & Stille, H. (2011). Filtration and penetrability of cement-based grout: Study performed with a short slot. *Tunnelling and Underground Space Technology*, 26(4), 548-559.
- Dumont, C. (1997). *Étude sur les coulis anti-lessivage pour l'injection*. Université de Sherbrooke.
- Evdokimov, P., Adamovich, A., Fradkin, L., & Denisov, V. (1970). Shear strengths of fissures in ledge rock before and after grouting. *Power Technology and Engineering (formerly Hydrotechnical Construction)*, 4(3), 229-233.
- Fomin, B. (1974). Grouting of construction joints in concrete dams at below-freezing temperatures. *Power Technology and Engineering (formerly Hydrotechnical Construction)*, 8(2), 117-120.
- Gallacher, D., & AECOM. (2010). *Remedial grouting works to two dams in Hong Kong*. Paper presented at the 16th Biennial Conference of the British Dam Society. Managing dams: Challenges in a time of Change, Edinburgh, UK.
- Heilmann, H. (1969). Beziehungen zwischen Zug-und Druckfestigkeit des Betons. *beton*, 2, 69.
- Holcim. (2008). The micro-cement design for oil well cementing, soil and rock consolidation, rehabilitation of damaged structures and high-performance solutions *Holcim Catalogue* (pp. 20). France: Holcim.
- Hydro-Quebec. (2008). Injection report of the plunging crack in the arch 6-7 of the Daniel-Johnson Dam. In D. a. C. W. Hydro-Quebec Report, Manicouagan Region (Ed.), (pp. 90). Manicouagan, Quebec, Canada.
- ICOLD-Committee-on-Concrete-Dams. (2008). The Physical Properties of Hardened Conventional Concrete in Dams. *International Committee on Large Dams*, 262.
- Jansen, R. B. (1988). *Advanced dam engineering for design, construction, and rehabilitation*: Kluwer Academic Publishers.
- Javanmardi, F., & Léger, P. (2005). Grouting of cracks in concrete dams: numerical modelling and structural behaviour. *Progress in Structural Engineering and Materials*, 7(4), 161-173.
- Kee, S. H., & Zhu, J. (2010). Using air-coupled sensors to determine the depth of a surface-breaking crack in concrete. *The Journal of the Acoustical Society of America*, 127, 1279.
- Khaloo, A. R., Shooreh, M. R. M., & Askari, S. M. (2009). Size influence of specimens and maximum aggregate on dam concrete: Compressive strength. *Journal of Materials in Civil Engineering*, 21(8), 349-355.
- Khan, A. A., Cook, W. D., & Mitchell, D. (1996). Tensile strength of low, medium, and high-strength concretes at early ages. *ACI Materials Journal*, 93(5).
- Khayat, K., Yahia, A., & Sayed, M. (2008). Effect of supplementary cementitious materials on rheological properties, bleeding, and strength of structural grout. *ACI Materials Journal*, 105(6).

- Kupfer, H. B., & Gerstle, K. H. (1973). Behavior of concrete under biaxial stresses. *Journal of the Engineering Mechanics Division*, 99(4), 853-866.
- Lapointe, R. (1997). *Contribution à l'étude des méthodes d'injection des fissures dans le béton*. M.Sc, Université McGill, Montréal, Canada.
- Larivière, R., Routhier, L., Roy, V., Saleh, K., & Tremblay, S. (1999). Grouting of the Cracks in the Arch 5-6 - Daniel-Johnson Dam (pp. 189 - 195): Hydro-Quebec.
- Lombardi, G. (1985a). *The role of cohesion in cement grouting of rock*. Paper presented at the 15<sup>th</sup> ICOLD Congress.
- Lombardi, G. (1985b). Some theoretical considerations on cement rock grouting. *Lombardi SA. N. Rif*, 102.
- Lombardi, G. (1996). Selecting the grouting intensity. *The International Journal on Hydropower & Dams, Volume Three, Issue Four*, 62-66.
- Lombardi, G. (1997). GIN principle revisited. *International water power & dam construction*, 49(10), 33-36.
- Lombardi, G. (1998). Idées Reçues sur l'Injection des Roches (pp. 1 - 16). Fontvieille-Minusio: École Polytechnique Fédérale de Lausanne.
- Lombardi, G. (2007). *Aspects Specifiques de l'Injection du Massif Rocheux*. Paper presented at the Symposium sur l'injection Rabat, Minusio.
- Lombardi, G. (2007). GIN again misunderstood. *GEOTECHNICAL NEWS-VANCOUVER*-, 25(2), 35.
- Lombardi, G. (2008). The Grout Line-Misunderstanding of GIN Confirmed. *Geotechnical News*, 26(2), 57.
- Lombardi, G., & Deere, D. (1993). Grouting design and control using the GIN principle. *International Water Power and Dam Construction IWPCDM*, 45(6).
- Mailvaganam, N. P. (1992). *Repair and protection of concrete structures*.
- Mnif, T. (1997). *Injectabilité des coulis de ciment dans des milieux fissurés*. Ph. D., Université de Sherbrooke, Sherbrooke, Québec, Canada.
- Morgan, D. (1996). Compatibility of concrete repair materials and systems. *Construction and building materials*, 10(1), 57-67.
- Nallathambi, P., Karihaloo, B., & Heaton, B. (1985). Various size effects in fracture of concrete. *Cement and Concrete Research*, 15(1), 117-126.
- Naudts, A., Landry, E., Hooey, S., & Naudts, W. (2003). Additives and Admixtures in Cement-based Grouts. *GEOTECHNICAL SPECIAL PUBLICATION*, 2, 1180-1191.
- Nguyen, V. H., Remond, S., & Gallias, J. L. (2011). Influence of cement grouts composition on the rheological behaviour. *Cement and Concrete Research*, 41(3), 292-300.
- Nianxiang, X., & Wenyan, L. (1989). Determining tensile properties of mass concrete by direct tensile test. *ACI Materials Journal*, 86(3).

- Nordtest. (2005). Wedge Splitting Test Method - Fracture Testing of Fibre-Reinforced Concrete (Mode I) (pp. 5). Stensberggata, Norway: Nordic Innovation Centre.
- Privileggi, V. (2012, Juin). *High Pressure Resins Injection of Piedra Del Aguila Dam. (Argentina)*. Paper presented at the Commission Internationale des Grands Barrages. Vingt Quatrième Congrès des Grands Barrages, Kyoto.
- Pronina, L., & Ashikhmen, V. (1996). Technology of repeated grouting of concrete dams. *Power Technology and Engineering (formerly Hydrotechnical Construction)*, 30(8), 456-461.
- Raphael, J. M. (1984). *Tensile strength of concrete*. Paper presented at the ACI Journal Proceedings.
- Rio, F., Fernandez, R., & Gonzalo, A. (2006). New Technology for the Grouting of Joints in a Vault Dam with Epoxi Resins. In B. e. al. (Ed.), *Dams and Reservoirs, Societies and Environment in the 21st Century* (Vol. 1, pp. 1003 - 1008). London: Taylor & Francis Group.
- Saleh, K., Tremblay, S., Lizotte, M., Larivière, R., Roy, V., & Routhier, L. (2003). Grouting of Daniel-Johnson Multiple Arch Dam. *Hydroplus - Hydroscience*(133), 62 - 65.
- Saleh, K., Tremblay, S., & Desbiens, V. (1997). Project 3D: Développement des Méthodes et de Produits s'Injection des Fissures dans des Structures en Béton. Recommandation sur les Méthodes, Produits et Équipements d'Injection. Manicougan, Québec: Direction Sécurité des Barrages et Direction Expertise et Support Technique Hydro-Québec.
- Saleh, K., Tremblay, S., Lizotte, M., Lariviere, R., Roy, V., & Routhier, L. (2002). Crack repair in concrete dams: identifying effective methods and materials. *Hydro Review*, 21(5), 40-49.
- Shah, S. G., & Kishen, J. (2010). Nonlinear fracture properties of concrete-concrete interfaces. *Mechanics of Materials*, 42(10), 916-931.
- Silvano, R., Frongia, F., Lombardi, G., Fonti, M., Ciciotti, F., & Gallavresi, F. (1997). Rehabilitation of the Flumendosa arch dam by epoxy grouting. *Hydropower and Dams*, 6, 62-67.
- Smoak, W. G. (1995). Lessons Learned at Deadwood Dam. *Concrete International-Design and Construction*, 17(3), 21-26.
- Stille, H., Gustafson, G., & Hassler, L. (2012). Application of New Theories and Technology for Grouting of Dams and Foundations on Rock. *Geotechnical and Geological Engineering*, 1-22.
- Tahmazian, B., Yeh, C.-h., & Paul, W. J. (1989). *Thermal Cracking and Arch Action in Daniel-Johnson Dam*. Paper presented at the International Symposium on Analytical Evaluation of Dam Related Safety Problems, Copenhagen.
- Turcotte, L., Savard, B., Lombardi, G., & Jobin, H. (1994). *The use of stable grout and GIN technique in grouting for dam rehabilitation*. Paper presented at the Annual Meeting Canadian Dam Safety Conference CDSA and CANCOLD.
- UDEC-(Universal-Distinct-Element-Code). (2000). User's Manual. Minneapolis, Minnesota, USA: Itasca Consulting Group Inc.

- United-States-Dept-of-the-Army. (1970). *Grouting Methods and Equipment*: Departments of the Army and the Air Force.
- US-Army-Corps-of-Engineers. (1995). Engineering and Design Chemical Grouting (pp. 34): Department of the Army.
- Vagn, J. C., Peter, T. C., & Paul, T. D. (2006). *Effect of Cement Characteristics on Concrete Properties, EB226, 2nd edition*. Skokie, Illinois, USA: Portland Cement Association.
- Veltrop, J., Yeh, C., & Paul, W. (1990). Evaluation of cracks in a multiple arch dam. *Dam Engineering*, 1(1), 5-12.
- Wang, H., & Song, Y. (2009). Behavior of mass concrete under biaxial compression-tension and triaxial compression-compression-tension. *Materials and Structures*, 42(2), 241-249.
- Willem, X., Courard, L., Darimont, A., Degeimbre, R., Marchand, J., Bissonnette, B., . . . Paradis, F. (2006). *Mix stability as a criterion for optimizing the granular composition to improve concrete durability-An application*. Paper presented at the 2nd International RILEM Symposium on Advances in Concrete through Science and Engineering.
- Wong, H. Y., & Farmer, I. (1973). Hydrofracture mechanisms in rock during pressure grouting. *Rock Mechanics and Rock Engineering*, 5(1), 21-41.
- Zhivoderov, V. (1993). Criteria for selecting and assigning optimal temperatures for grouting joints. *Power Technology and Engineering (formerly Hydrotechnical Construction)*, 27(9), 532-539.